Title

Cellular and molecular mechanisms of corneal lymphangiogenesis and valvulogenesis

Author

Kang, Gyeong jin

Publication Date

2018

Cellular and Molecular Mechanisms of Corneal Lymphangiogenesis and Valvulogenesis

By

Gyeong Jin Kang

A dissertation submitted in partial satisfaction of the

requirements for the degree of

Doctor of Philosophy

in

Vision Science

in the

Graduate Division

of the

University of California, Berkeley

Committee in charge:

Professor Lu Chen, Chair

Professor Suzanne Fleiszig

Professor Sona Kang

Summer 2018

Abstract

Cellular and Molecular Mechanisms of Corneal Lymphangiogenesis and Valvulogenesis

by

Gyeong Jin Kang

Doctor of Philosophy in Vision Science

University of California, Berkeley

Professor Lu Chen, Chair

The cornea is the outermost layer of the eye serving as the first barrier from the outside environment which plays a crucial role in a clear vision. It is maintained by keeping transparency and avascularity under the normal state. This nature makes the cornea an ideal site to study lymphangiogenesis (LG), new lymphatic vessel growth, that can be induced by inflammation and assessed without any background vessels. The lymphatic vessels have long been neglected over blood vessels due to its invisibility, but its importance and involvement in inflammation, cancer metastasis, and transplant rejection are now well known since the discovery of several lymphatic-specific markers in recent years. Another important event that occurs during LG is valvulogenesis (VG). Previous studies from our lab have shown that lymphatic vessels develop luminal valves in the cornea during LG, and these valves express integrin alpha 9 (Itga-9) that plays a critical role in directing lymph flow.

My study consists of three parts: 1) to investigate the dynamic changes of LG and VG during corneal inflammation. This was revealed by our newly developed intravital imaging system; 2) to assess the role of VG itself or VG and LG together in corneal transplant rejection; and 3) to explore the cellular origin of corneal lymphatic endothelial cells that comprises lymphatic vessel walls.

First, using the intravital imaging technology, I demonstrated the multifaceted dynamics of LG and VG associated with corneal transplantation, from the initiation to regression phases, and reported several novel and critical phenomena and mechanisms that couldn't be detected by conventional *ex vivo* immunohistochemistry.

Secondly, I investigated corneal transplant rejection reaction after blocking VG alone or in combination of LG. The results showed that anti–Itga-9 treatment alone suppressed corneal VG after transplantation. While this treatment did not affect LG, it promoted corneal graft survival in the low-risk setting. This study has provided the first evidence

on the critical role of VG in mediating graft rejection. Furthermore, I have shown that combined blockade of VEGFR-3 (vascular endothelial growth factor receptor-3) and Itga-9 significantly suppressed both LG and VG after corneal transplantation, and this treatment led to a markedly promoted survival rate in the high-risk setting.

Lastly, I have provided the first *in vivo* evidence showing that transplanted bone marrow (BM) derived cells integrated into the newly formed lymphatic vessels in inflamed host corneas with the live imaging system.

In summary, my study reveals novel molecular and cellular mechanisms that contribute to LG and VG in the cornea. It is our hope that understanding these mechanisms would lead to novel therapies not only for corneal transplant rejection and inflammation, but also for lymphatic-related disease occurring outside the eye, such as cancer metastasis and lymphedema.

Acknowledgments

First of all, I'd like to thank my Lord for your immutable love, pouring strength when I was down, and giving me true inspiration. I would also like to express the deepest appreciation to all the people stayed by my side throughout this long journey.

I would like to express my sincere gratitude to my supervisor Dr. Lu Chen for her continuous support, patience, motivation, and vast knowledge helped me to carry out this assignment. I also thank my committees; Dr. Suzanne Fleiszig, Dr. Sona Kang, and Dr. Song Li for their support with expertise in the field and wisdom as scientists.

I would like to thank my lab mates; Dr. Guangyu Li, Dr. Don Yuen, Dr. Roberto Sessa, Dr. Narae Lee, Dr. Ying Wen, Dr. Liwei Zhang, Dr. Tatiana Ecoiffier, and Dr. Eda Altiok, who have been the best collaborator and stabilizer when I was in a panic in the lab. I also thank my undergraduate assistant researchers: Anna Sadovnikova, Jenny Wu, Grace Poon, Valeri Su, and Anna Gong who were willing to give their best.

It would have not been possible to finish my journey without endless encouragements with hugs and kisses of Vision Science Graduate Program: especially Inez Bailey, Linda Schmidtz, Heather Iwata, Carissa Caloud, my fellow students: Dr. Aaron Sullivan, Dr. Christy Sheehy, Dr. Diane Nava, Dr. Christina Gambacorta, Dr. Brent Parsons, and Jessica Wei.

Finally, I'd like to give my biggest thank to my family: my husband, best friend, and a scientist Dr. Kyung Han Song, my mom Dr. Yun Young Yang, my grandfather Dr. Sang Hyun Yang, my grandmother Eul Woo Jeong, and my lovely kids Lucas and Aiden, for their unconditional support, sacrifice, and love.

Table of Contents

List of Figures and Tables

1. INTRODUCTION

1.1. ANATOMY AND PHYSIOLOGY OF THE EYE AND THE CORNEA

The eye is a highly specialized organ that receives light and transmits visual information to the brain. Structures in the eye are necessary for focusing and transmitting the light on to the retina to form visual signals or for nourishing and supporting the tissues of the eye (Fig. 1). For example, the sclera protects the eye from external forces and maintains its shape; the ciliary body regulates lens refractive power; the choroid provides oxygen and nutrients to the retina; and the retina detects light and converts it into electro-chemical impulses. Visual signals travel to the brain via the optic nerve.

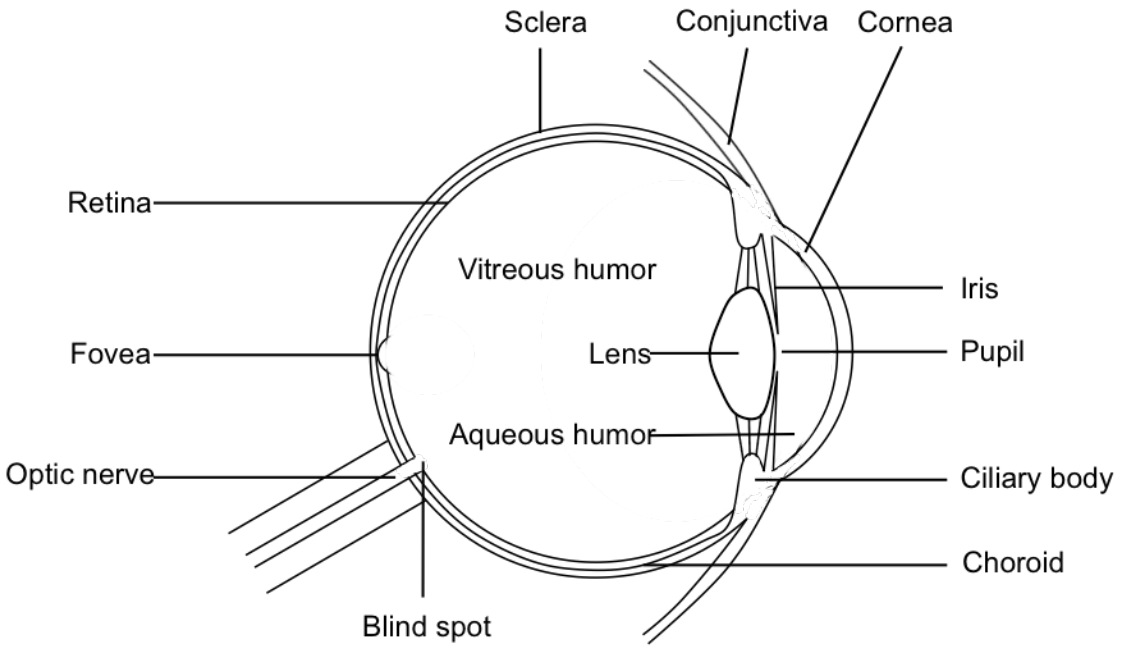

Figure 1. Schematic diagram of the human eye. (modified from http://igbiologyy.blogspot.com/2014/03/88-structure-and-function-of-eye-rods.html)

The cornea is the first barrier of the eye against infectious, toxic, and mechanical damage from the outside environment. It borders the sclera at the limbus. It is also an important refractive tissue of the eye[1]. The shape of the cornea is horizontally oval, convex, and aspheric and its thickness increases in periphery in human[2]. To provide optical clarity, the cornea maintains avascularity, uniform structure, and relatively dehydrated state. The human cornea has five recognized layers as follows (Fig.2).

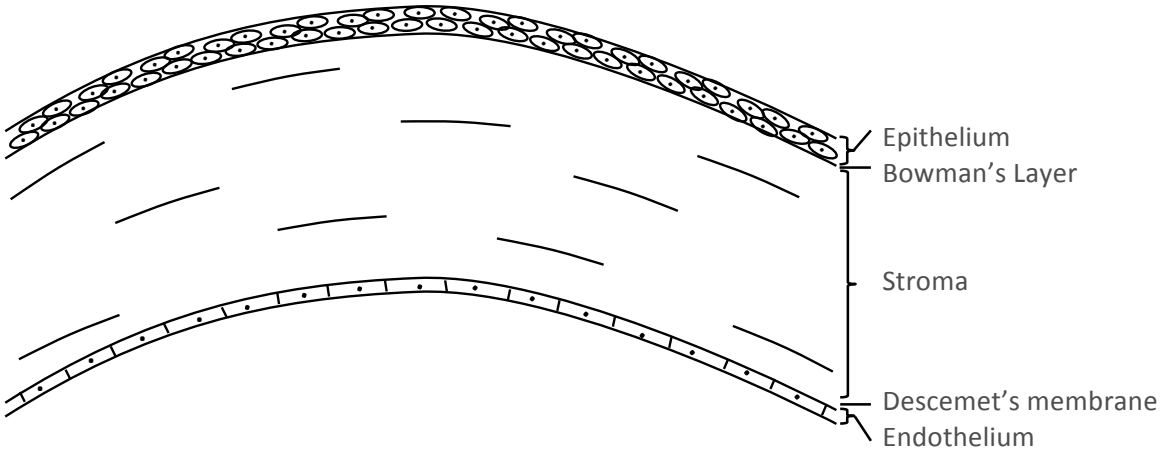

Figure 2. Cross-sectional view of the corneal layers.

1.1.1. Epithelium

The epithelium is a non-keratinized stratified squamous layer comprising about 10 percent of the entire thickness in human. It is a densely innervated tissue that is extremely sensitive to pain. It also serves as an integral part of the tear film–cornea interface[3]. The cells in the exposed layer are shed constantly and replenished by cells from the basal layer[4]. Cells in the epithelium are tightly held together to prevent tears from entering the intercellular spaces and toxins and microbes from entering inner corneal layers. The lateral membrane of the cells has desmosomes and basal cells are tightly attached to basement membrane by hemidesmosomes and anchoring filaments[5]. Corneal epithelium contains no melanocytes for transparency but has Langerhans cells for immune protection.

1.1.2. Bowman's layer

Bowman's layer lies between the epithelium and the stroma and terminates at the limbus. It is an acellular condensate that is mostly composed of tightly woven collagen fibrils. Its front surface is well-delineated and separated from the epithelium by the thin basal lamina and the back surface merges with the stroma. The main function of this layer is maintaining the shape of the cornea[3].

1.1.3. Stroma

The stroma makes up the vast majority of the cornea and it maintains the shape of the globe together with the sclera. It consists predominantly of collagenous lamellae and their precise organization contributes to the characteristic transparency of the cornea[6]. Each layer of the lamella is arranged at right angles relative to fibers in adjacent lamella[7].

Highly organized with the regular diameter and spacing of the collagen fibers, lamellae reduce forward light scatter[8] and mechanical strength of the cornea as well.

The major cell type of the stroma is keratocyte. They are flattened, modified fibroblasts lying between the lamellae. Keratocytes play important role in maintaining the extracellular matrix (ECM) environment and stromal homeostasis. Keratocytes are arranged in a corkscrew pattern and connected by gap junctions to their adjacent cells[3]. Inside corneal stroma, there are other types of cells as well, such as macrophages and dendritic cells. During a pathological stimulation such as inflammation, the number of these cells increases. This is also the site where new vessels (blood and lymphatic) will be developed, as stated later in this section.

1.1.4. Descemet's membrane

Descemet's membrane is a thin, modified basement membrane of the corneal endothelium that lies behind the stroma. It is a homogenous layer that is rich in basement membrane glycoproteins[3].

1.1.5. Endothelium

The endothelium is a one-cell layer on the posterior surface of the cornea. The endothelial cells adhere on Descemet's membrane by numerous hemidesmosomes and they form a hexagonal array. The lateral surface of cells in this layer is extensively interdigitated with gap and tight junctions. They are metabolically active with a number of mitochondria. This is important for maintaining a relative dehydrated state of the cornea and thereby its transparency[3,9]. The endothelium actively pumps ions out of the stroma via Na+, K+-ATPase pump[10] and the intracellular carbonic anhydrase pathway. Unlike the epithelium, cells in the endothelium have low regenerative capacity and dead cells are compensated by spreading of the adjacent cells which reduces overall cell density and affects fluid balance as well.

1.1.6. Vascular supply and avascularity of the cornea

The cornea is devoid of both blood and lymphatic vessels under normal condition. This unique feature of avascularity is essential in providing corneal transparency, which is controlled by the natural balance of local pro- and anti-angiogenic or –lymphangiogenic mediators[11]. It also plays a role in immune privilege, a concept in which certain transplanted tissues undergo less destructive immunological rejection processes. Loss of corneal avascularity and integrity, in contrast, leads to corneal opacity and diminished visual acuity.

1.2. CORNEAL LYMPHANGIOGENESIS AND VALVULOGENESIS

Corneal lymphangiogenesis (LG, the formation of new lymphatic vessels) can be induced by an inflammatory, infectious, chemical, traumatic, or toxic insult. Proof of LG in the cornea has been hindered due to the invisibility of lymphatics. This has recently changed

with the discovery of specific lymphatic markers such as vascular endothelial growth factor receptor-3 (VEGFR-3), LYVE-1 (lymphatic vessel endothelial hyaluronic acid receptor-1), podoplanin, and Prox-1 (prospero homeobox protein-1; the master control gene for lymphatic development)[12-14]. LG is now known for its involvement in a wide array of diseases and pathological conditions inside and outside the eye, which include but are not limited to inflammation, infection, cancer metastasis, and transplant rejection[15-17].

The lymphatic system plays essential roles in immune surveillance, body fluid homeostasis, and dietary fat and vitamin absorption. The formation of lymphatics begins with Prox-1 gene expression. Endothelial cells expressing this gene bud from veins and differentiate as lymphatic endothelial cells (LECs), which leads to the formation of the lymphatic channels. Without these budding endothelial cells expressing the homeobox gene Prox-1, the lymphatic system fails to develop.

It has recently revealed that lymphatic vessels develop luminal valves as LG progresses, and these valves play a crucial role in guiding the flow of the lymph inside the vessels, which contains immune cells and antigens for immune responses[18,19]. Since the cornea offers an ideal site for pathological LG research due to its accessible location, transparent nature, and alymphatic status under normal condition, it is exceptionally straightforward and accurate to assess pathological LG and valvulogenesis (VG, the formation of new lymphatic valves) without any background interference in this tissue[16].

1.3. ROLE OF LYMPHANGIOGENESIS IN MEDIATING CORNEAL TRANSPLANT REJECTION AND ITS MANAGEMENT VIA MOLECULAR TREATMENT

Corneal transplantation is one of the most successful and frequently performed tissue transplantations in the world. The paucity of potential antigen presenting cells, such as dendritic cells, and the avascular nature of the cornea are of crucial importance to the success of corneal grafting. However, the success rate of transplantation largely depends on the state of recipient cornea. When grafted on avascular and non-inflamed bed (low-risk), more than 90% remain accepted after 2 years[20], while rejection rate of vascularized and inflamed bed (high-risk) can be 50-90%[21,22] despite maximal immune suppression. This is because neovascularized cornea has its immune privilege compromised and therefore results in graft failure due to immune reaction[16,23-25]. Unfortunately, most recipients of corneal transplantation are already traumatized by inflammation, infection, chemical burn, or transplantation failure putting them into high-risk. Therefore, finding a therapeutic protocol to resolve this problem is in demand.

The immune reflex arc of transplant rejection is consisted of two components. Lymphatic vessels serve as an afferent arm to transport antigens and antigen presenting cells from the site to the draining lymph node, where blood vessel serves as an efferent arm to transport primed T cells from the regional lymph nodes to the targeted graft[16,23,24,26]. Yamagami et al. reported that surgical interfering of the lymphatic pathway by the

removal of draining lymph nodes promoted 100% and 90% of transplant survival in low- and high-risk settings, respectively [27,28]. However, surgical lymphadenectomy for promoting transplant survival is not practical in human patients. Previous studies from our lab and other researchers instead selectively blocked lymphatic vessels and demonstrated that lymphatic vessels, not blood vessels, are the mediator of immune rejection against donor tissue[29,30]. Collectively, studies have shown that transplantation immunity can be modulated by a molecular blockade of the lymphatic pathway[30-34], and lymphatic vessels have emerged as key modulators for the development of new therapeutic strategies.

1.3.1. Anti VEGFR-3 treatment

Members of the VEGF family (VEGF-A, C, and D) have been recognized as involved in corneal angiogenesis and lymphangiogenesis[35-38]. VEGF-C/VEGFR-3 signaling pathway, especially, is essential for lymphatic vessel growth[39,40]. The master control gene Prox1 upregulates the gene encoding the tyrosine kinase receptor VEGFR-3 on LECs. It is activated by its ligands VEGF-C and VEGF-D, and this activation leads to the proliferation, migration, and survival of LECs[41]. Previous reports have found that blockade of VEGFR-3 after transplantation in low- or normal-risk corneas promoted graft survival by suppressing donor-derived cell trafficking to draining lymph nodes[42-44].

1.3.2. Anti Itga-9 treatment

Integrin alpha 9 (Itga-9) belongs to the integrin family that mediates cell-cell and cell-matrix interactions[45]. Previous studies from our lab have shown that this molecule is highly expressed on newly formed lymphatic valves in the cornea[18,19], and its gene knockdown can inhibit the functions of human dermal LECs in vitro, such as proliferation, adhesion, migration, and tube formation. Our lab has also demonstrated with a suture placement model that Itga-9 blockade can suppress inflammatory VG in a brief 2-week study[46]. It is yet to be determined whether an intervention of VG can modulate transplant survival, which is a focus of this study.

1.4. CELLULAR ORIGIN OF CORNEAL LYMPHANGIOGENESIS

The origin of LECs during development has been a long debate for over a century. In 1902, Sabin proposed that LECs derived from the cardinal vein through remodeling and sprouting (LG)[47]. An opposing model has been proposed by Huntington and McClure in 1910 proposing that primary lymph sacs could arise in the mesenchyme by concrescence of discontinuous and independent lymph vesicles (lymphvasculogenesis)[48]. Both models have been supported by recent studies and are still in debate[49-52].

Like LG during development, the origin of LECs in adult is in debate. Postnatal LG has long been thought to be sprouted from pre-existing lymphatic vessels[39,53-56]. However, compelling evidences from recent studies have shown that bone marrow (BM)-derived cells, which have known to be involved in LG by producing and secreting lymphangiogenic cytokines (VEGF-C and VEGF-D) upon inflammatory activation to

induce local sprouting of pre-existing LECs[57-59], may comprise a small fraction of LECs in the newly formed lymphatic vessels[60-62]. Many evidences of lymphatic endothelial cell progenitors (LECPs) present in bone marrow[62-68], peripheral blood[60,69-73], and even in tissue[61,74,75] have been reported recently. LECPs possess tremendous potential for a better understanding of LG and precise control of LG in pathological context for a therapeutic protocol.

In the cornea, lymphatics have been observed to arise within the cornea which then connect to the limbal lymphatic vessels and also by growing from the limbal lymphatics, suggesting the possibility of lymphvasculogenesis in the cornea. Presence of BM-derived cells in the cornea and its integration into corneal lymphatic network after seeding *in vitro* induced BM cells under tumor or LPS treatment has been reported[62,76,77], but direct evidence of corneal resident cells and/or BM-derived cells serving as a structural contributor to lymphatic endothelial walls and its transition into newly formed LECs *in vivo* yet has to be examined.

1.5. PURPOSE OF THE STUDY

This study aims to reveal the cellular and molecular mechanisms of corneal LG and VG in various contexts. Specifically, I investigated time course intravital images of LG and VG within the cornea using our newly developed live imaging system and reported several new phenomena and mechanisms that cannot be detected by conventional ex vivo study, including VG initiated from inside the limbal vessels, lymphatic elongation achieved by stalk cell lateral migration, lymphatic pruning from vessel tips, and lymphatic regression within late stage vessels. These findings not only offer novel insights into pathological LG and VG, but also provide critical information for further investigation and modulation of LG and LG-related diseases at various stages.

Next, I evaluated corneal transplant survival after VG suppression via molecular blockade of Itga-9 Itga-9 single treatment was performed to determine (1) whether Itga-9 blockade can be used as a new strategy to interfere with VG induced by transplantation; and (2) whether VG plays a critical role in transplant rejection, which to date, there has been no report on this aspect; My results showed that this strategy can be used to inhibit VG without interfering LG and this treatment alone can be used to promote graft survival in the low-risk setting. I further demonstrated that a combined blockade of VEGFR-3 and itga-9 could suppress both LG and VG and thereby markedly promote graft survival in the high-risk setting. What makes this study more significant is that I used intravital imaging system and anterior segment optical coherence tomography (OCT) to closely monitor the effects of the pharmaceutical intervention.

Taking advantage of intravital imaging, I also investigated whether corneal LG can arise from BM-derived origin and confirmed this by transplanting GFP+ whole bone marrow cells into Prox-1 tdTomato recipients.

Taken together, these findings not only offer novel insights into pathological LG and VG, but also provide critical information for modulation of LG-related diseases at various stages and in different settings. The current regimens of corticosteroids are of limited efficacy and also associated with many side effects, such as opportunistic infection, glaucoma, and cataract. Results from my studies may offer lymphatic-specific targeting for precision medicine.

2. MATERIALS AND METHODS

2.1. MICE

Prox-1 GFP hybrid mice were generated by cross breeding between wildtype C57BL/6 mice (Taconic Farms, Germantown, NY, USA) and Prox-1 GFP mice of FVB/N background[78] (University of Southern California). Prox-1 tdTomato in B6;129S background (The Jackson Laboratory) mice were also used as corneal transplant recipients from Prox-1 GFP donors. Six- to 8-week-old male BALB/c and C57BL/6 mice (Taconic Farms, Germantown, NY, USA) were used in Itga-9 blockade study, and ten- to thirteen-week-old male BALB/c donor mice and eight- to twenty one-week old Prox-1 GFP recipient mice were used in combined blockade study[79]. For bone marrow transplantation, β-actin eGFP donor mice and 9-week-old C57Bl/6 recipient mice were used. Mice were anesthetized using a mixture of ketamine, xylazine, and acepromazine (50mg, 10mg, and 1mg/kg body weight, respectively) for each surgical procedure. All mice were treated according to the ARVO Statement for the Use of Animals in Ophthalmic and Vision Research and all protocols were approved by the Animal Care and Use Committee, University of California, Berkeley.

2.2. *IN VIVO* MODELS

2.2.1. Corneal suture placement

The procedure was performed as previously reported[80]. Briefly, 11-0 nylon sutures (AROSurgical, Newport Beach, CA) were placed intrastromally without penetrating into the anterior chamber.

2.2.2. Corneal micropocket implantation

The procedure was performed as previously reported[81]. Corneal micropocket was created 1.0mm apart from limbal vascular arcade using a modified von Graefe Knife and slow-release pellet was implanted into the pocket. The pellet was made of sucralfate (Sigma Aldrich, St. Louis, MO) and hydron polymer (Sigma Aldrich) containing 400ng VEGF-C (R&D Systems, Minneapolis, MN) and left in place for 9 days.

2.2.3. Corneal transplantation and in vivo assessment of grafted corneas

Standard orthotopic corneal transplantation was performed[30]. Briefly, the central cornea of the donor was marked with a 2-mm diameter micro-curette (Katena Products Inc., Denville, NJ) and excised with Vannas scissors (Storz Instruments Co, San Dimas, CA). The recipient graft bed was prepared by excising a circular 1.5-mm area in the central cornea. The donor button was placed onto the graft bed and secured with eight interrupted 11-0 nylon sutures (AROSurgical). Antibiotic ointment was applied at the end of the surgery. After the transplantation surgery, all eyes were first examined on day 3 and corneal sutures were removed on day 7, as described previously[30]. Grafts were evaluated by ophthalmic slit-lamp biomicroscopy twice a week for 8 weeks according to

the standard scheme. Basically, the degree of graft opacification was graded between 0 (clear and compact graft) to 5+ (maximal opacity with total obscuration of the anterior chamber). Grafts with an opacity score of 2+ or higher after 3 weeks or an opacity score of 3+ or higher at 2 weeks were regarded as rejected.

2.2.4. Bone marrow transplantation

Whole bone marrow cell transplantation was performed to observe the migration of BM-derived cells into the mouse cornea. β-actin eGFP mice were sacrificed and BM cells were obtained by flushing the femurs and tibias with sterile Dulbecco's Modified Eagle Medium (DMEM). The BM cells were washed several times in sterile DMEM, filtered through a nylon mesh (pore size, 40μm), counted, and resuspended in PBS at 1 $\times 10^7$cells/mL. Each C57Bl/6 recipient mice mouse was lethally irradiated with 9 Gy in two equal doses delivered 4 h apart. About 1×10^6 BM cells harvested from donor β-actin eGFP mice in a volume of 100 μl PBS were injected into the tail vein of recipient mice. These BM cell transplant recipients were then maintained under special pathogen-free conditions, and successful BM cell transplantation was confirmed by the identification of GFP+ cells in the cornea at 3 weeks after transplantation. 9 successfully BM transplanted mice were used for further experiment.

2.2.5. Intravital imaging

The procedure was performed as we previously reported[19,82]. The samples were imaged with a customized imaging system including an adjustable eye and head stage holder and the Axio Zoom.V16 microscope (Carl Zeiss AG). Digital pictures were taken under FITC excitation light, Cy3 excitation light, or LED bright field light. For Supplementary Video 1, series of time-lapse images were taken in a time frame of 1 image per 10second. A total of 13 images taken within 120seconds were streamed to 4seconds with the NIH Image J software as reported previously[82].

2.2.6. Central Cornea Thickness Measurement With Anterior Segment Optical Coherence Tomography

Anterior segment OCT images were analyzed as reported previously[83]. Briefly, three repeated volumetric images for each cornea were acquired every week up to 8 weeks post transplantation with Anterior segment OCT (Visante OCT MODEL 1000; Carl Zeiss Meditec, Dublin, CA, USA) and central cornea thickness (μm) was measured as the distance from epithelium to endothelium, at the point where a vertical line was orthogonal to the anterior corneal curvature. Mean measure of three frames was averaged for statistical analysis.

2.2.7. Pharmaceutical intervention

VEGFR-2 treatments were performed as previously reported[84]. Mice after one suture placement at 12 o'clock were randomized to receive intraperitoneal administration of

VEGFR-2 neutralizing antibody (800μg, DC101; Eli Lilly and Company, New York, NY) or PBS on Day 0 and Day 4 post-suturing.

Itga-9 treatments were performed as previously reported[46]. The recipient mice were randomized to receive subconjunctival injections of either hamster anti-mouse Itga-9 antibody (6.4 μg; kindly provided by Toshimitsu Uede, MD, PhD, Hokkaido University, Hokkaido, Japan) or its isotype control hamster IgG (Jackson ImmunoResearch, West Grove, PA, USA), as reported previously[46]. Subconjunctival injection was performed twice a week on the day of transplantation and thereafter up to 8 weeks after the surgery.

Combined treatments were performed as follow. After surgery, mice were randomized to receive either subconjunctival administrations of neutralizing antibodies of Itga-9 (3.4 μg; kindly provided by Dr. Yokosaki (Hiroshima University, Japan) every the other day and systemic administration of VEGFR-3 (700 μg; mF4–31C1; kindly provided by ImClone Systems Incorporated, Eli Lilly and Company, New York, NY) twice a week or subconjunctival and systemic injection of PBS controls in the same volume from the day of transplantation and thereafter up to 8 weeks. An antibiotic ointment was placed on the corneal surface following injections.

2.3. *EX VIVO* METHODS

Primary and secondary antibodies are listed in Table 1. The experiments were performed as previously reported[18,19,80]. Briefly, whole-mount full thickness wild type corneas were fixed in acetone or 4% PFA for Prox-1 GFP transgenic mouse cornea and sequentially incubated with primary and secondary antibodies (Table 1). Samples were covered with Vector Shield mounting medium (Vector Laboratories, Burlingame, CA) and examined by an AxioImager M1 epifluorescence deconvolution microscope with AxioVision 4.8 software (Carl Zeiss AG, Göttingen, Germany).

Table 1. List of antibodies and manufacturers

Primary antibody	Secondary antibody
rabbit anti-mouse LYVE-1 (Abcam)	FITC-conjugated donkey anti-rabbit (Jackson ImmunoResearch Laboratories)
	Cy3-conjugated donkey-anti-rabbit (Jackson ImmunoResearch Laboratories)
goat anti-mouse LYVE-1 (R&D Systems)	AMCA-conjugated donkey anti-goat (Jackson ImmunoResearch Laboratories)
goat anti-mouse Itga-9 (R&D Systems)	Cy3-conjugated donkey anti-goat (Jackson ImmunoResearch Laboratories)
rabbit anti-mouse Prox-1	Cy3-conjugated donkey-anti-rabbit (Jackson ImmunoResearch Laboratories)

2.4. QUANTIFICATION AND STATISTICAL ANALYSIS

2.4.1. Lymphatic vessel and valve quantification

For chapter 3.1, Lymphatic density in the prox-1 GFP cornea after transplantation from 11 to 1 o'clock was graded and analyzed using the NIH Image J software[84]. Individual lymphatic vessels were highlighted and added together to generate a density score measured in pixels for each sample. The number of branching points and lymphatic valves from the same area were counted for each sample. The experiments were repeated twice with 5 mice in each group of the study. For VEGFR-2 treated prox-1 GFP cornea, lymphatic density within 9 to 3 o'clock area was graded and analyzed in the same way. The experiments were repeated twice with a total of 6 mice in the treatment and 7 mice in the control groups.

For chapter 3.2.1, the analysis for lymphatic vessel and valve was performed as reported previously[19,37,46,85,86]. Briefly, for LG evaluation, LYVE-1+ vascular structures were analyzed by ImageJ software (http://imagej.nih.gov/ij/; provided in the public domain by the National Institutes of Health, Bethesda, MD, USA). The lymphatic invasion area was normalized to the total corneal area to obtain a percentage coverage score for each sample. The total corneal area was measured by outlining the innermost lymphatic vessels of the limbal arcade, and lymphatic invasion area was determined by tracing out the contours of the LYVE-1+ lymphatic network inside the cornea. Additionally, the cornea was divided into four equal quadrants in reference to the vertical midline passing through the 6- and 12-o'clock positions, and the nasal and temporal quadrants were used for analysis of polarized lymphatic vessel distribution for each sample[19]. Luminal valves also were evaluated and focal Itga-9+/LYVE-1− areas running along the length of the LYVE-1+ vessels were identified as valves and quantified for each sample. The percentage scores were obtained by normalizing to the means of control condition that were defined as being 100%[46,85].

For chapter 3.2.2, LG was evaluated by quantifying Prox-1+ vascular structures in two different zones of the cornea graded every week up to 8 weeks after transplantation. The quantification of vessels in the host beds was based on two primary parameters. One was the circumferential extent of 12 areas around the clock. A score of 1 was given to each area if the vessels were present in the sector. The other was the centripetal growth of the longest vascular frond in each area. A grade between 0 (no growth) and 2 (at the grafting border for host bed vessel quantification or at the center of the cornea for donor button vessel quantification) was given to each area. Scores for each area were then summed to derive the final index (range, 0–24; maximal score, 24 = 2 x 12). Vessels in the donor button were quantified based on their presence around 12 clocks (range, 0–12) (Fig 15A). Luminal valves were also evaluated every week up to 8 weeks after transplantation.

2.4.2. Statistical analysis

The results are reported as mean±SEM. Student *t*-test, Mann-Whitney *U* test, and one-way ANOVA were used to determine the significance levels between the groups. Corneal

graft survival was assessed by Kaplan-Meier survival curves. The differences were considered statistically significant when $p<0.05$ using Prism software (GraphPad, La Jolla, CA). The association analysis was performed by the linear mixed model built with the R Studio platform (R Studio Inc., Boston, MA, USA) using the nlme R package. Corneal graft survival from combined treatment was assessed by cox regression models built with the R Studio platform (R Studio Inc., Boston, MA, USA) using the nlme R package and the differences were considered statistically significant when $p<0.05$.

3. RESULTS

3.1. INTRAVITAL IMAGING REVEALS DYNAMICS OF LYMPHANGIOGENESIS AND VALVULOGENESIS

From: Kang, G. J., Ecoiffier, T., Truong, T., Yuen, D., Li, G., Lee, N., Zhang, L., and Chen, L. Intravital Imaging Reveals Dynamics of Lymphangiogenesis and Valvulogenesis. Scientific Reports, (2016).

3.1.1. Results

3.1.1.1. Corneal intravital imaging in modified Prox-1-GFP mice

Prox-1-GFP mice in FVB/N background have been reported to faithfully recapitulate the expression of Prox-1 in lymphatic endothelial cells[78]. However, they are not suitable for live imaging in the cornea due to the constitutive expression of Prox-1 in lens epithelium. As shown in Fig 3a, to enable intravital imaging of lymphangiogeneic process within the cornea, we cross-bred the founder Prox-1-GFP mice in FVB/N background with wildtype C57BL/6 mice. The highly pigmented iris in black C57BL/6 mice, an anatomical structure located between the cornea and lens, blocks lens interference and hence allows for corneal imaging.

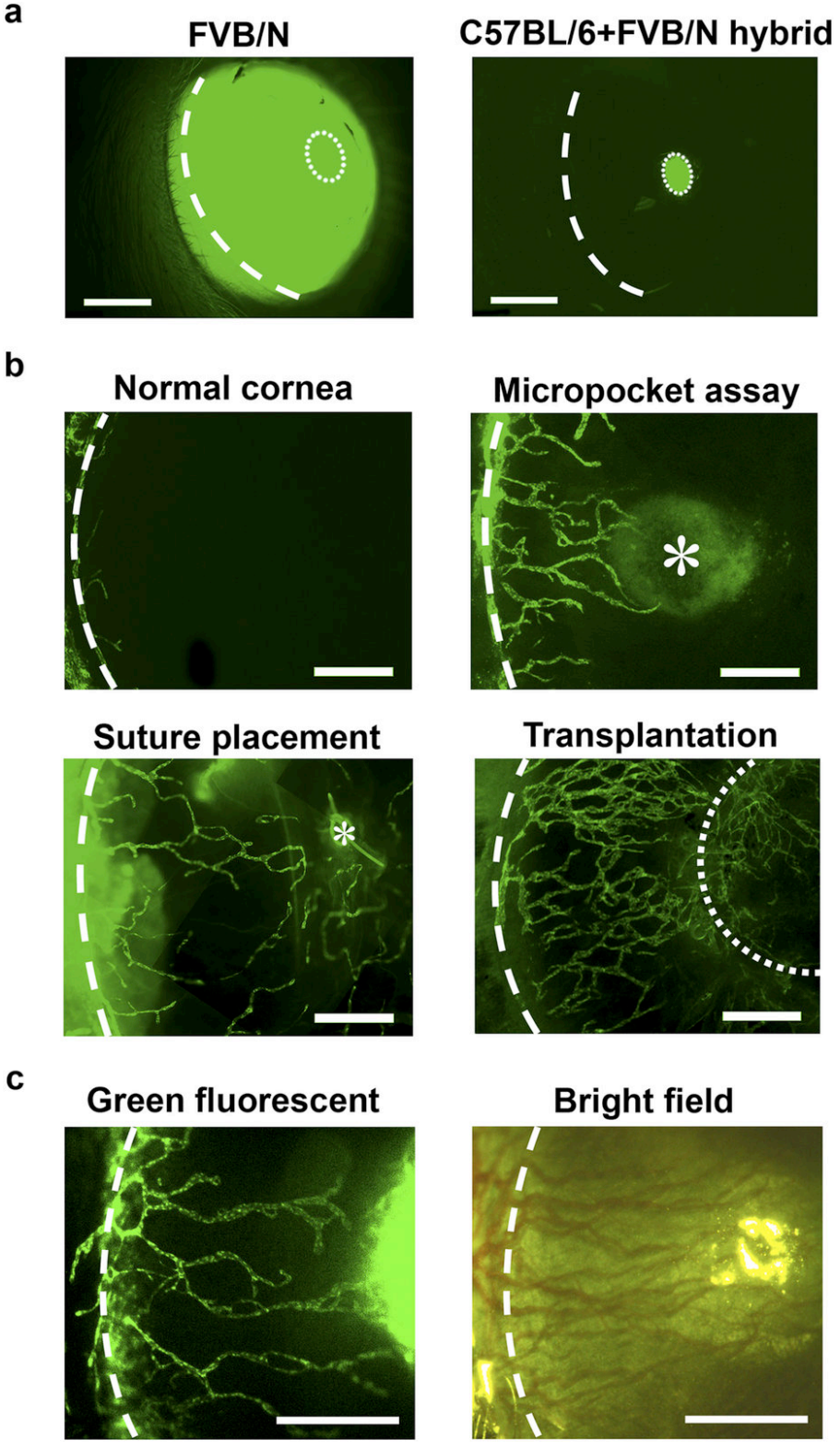

Figure 3. Corneal intravital imaging in modified Prox-1-GFP mice showing lymphatic vessels induced by various insults. **(a)** Intravital images of Prox-1-GFP mice of the FVB/N background and FVB/N-C57BL/6 hybrid showing high fluorescence signals from lens epithelium were blocked by the pigmented iris in the hybrid. Scale bars: 1mm. **(b)** Intravital images demonstrating newly formed lymphatic vessels induced by various pathological insults. Scale bar: 500μm. **(c)** Intravital images of the same cornea post-suturing showing newly formed lymphatic vessels (green) visualized under green fluorescent light and blood vessels (red) under bright field light. Scale bar: 500μm. Dashed line: demarcation of the limbus between the cornea and conjunctiva; Dotted line: pupil margin **(a)** or graft-host border **(b)**; Asterisk: site of VEGF-C pellet implantation or suture placement **(b)**.

3.1.1.2. Intravital imaging visualizes lymphangiogenesis induced by various insults

We next demonstrated that the modified transgenic mouse model can be used to visualize corneal LG induced by various pathologic insults, including micropocket implantation of vascular endothelial growth factor-C (VEGF-C), suture placement, and transplantation (Fig. 3b). These are the most commonly used LG models with the cornea[16,87]. We also demonstrated that both lymphatic and blood vessels can be detected in the cornea under fluorescein isothiocyanate (FITC) green fluorescent excitation source or LED with bright field (Fig. 3c).

To confirm the Prox-1 GFP positive vessels detected in the corneas of the transgenic hybrid mice were lymphatics, we performed immunofluorescent microscopic analysis using specific antibodies against LYVE-1, the most widely used marker for lymphatic identification. Our data verified the co-localization of Prox-1 GFP and LYVE-1 signals on corneal lymphatic vessels (Fig. 4a). Additionally, we also observed Prox-1 GFP signal on the luminal valves inside lymphatic vessels, and further immunofluorescent microscopic analysis validated their co-localization with integrin alpha-9 (Itga-9), the specific marker for lymphatic valves (Fig. 4b).

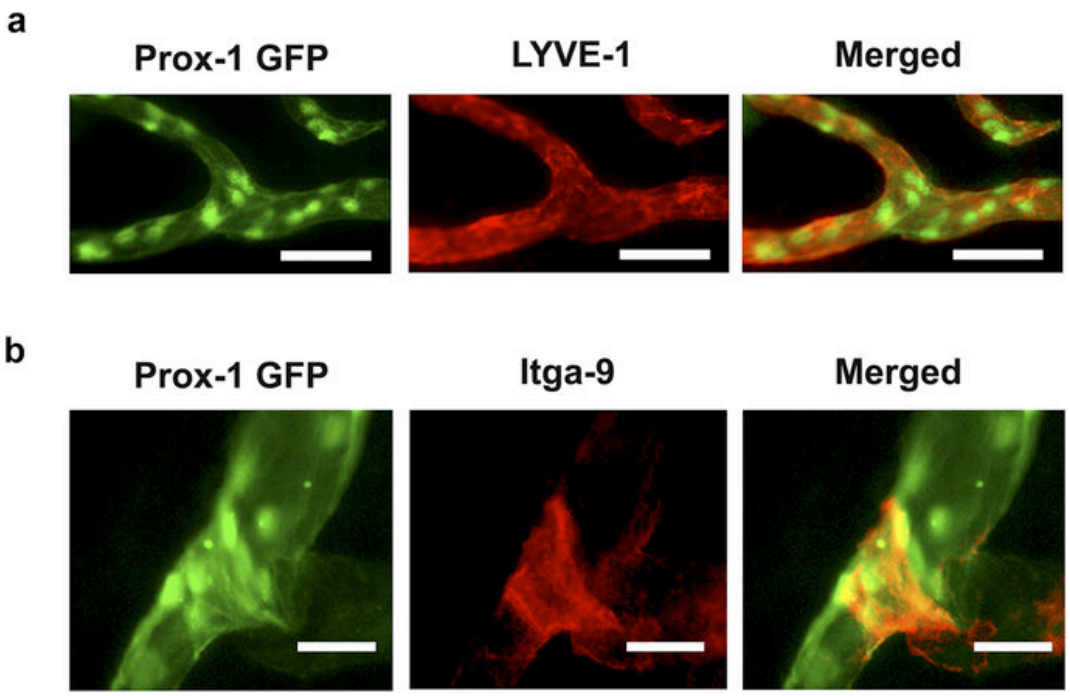

Figure 4. Immunofluorescent microscopic analysis confirming Prox-1 GFP signals identify lymphatic vessels and valves in the cornea. **(a)** Immunofluorescent microscopic images showing co-localization of Prox-1 GFP signal (green) and LYVE-1 staining (red) along newly formed lymphatic vessels in the inflamed cornea. Scale bars: 50μm. **(b)** Immunofluorescent microscopic images showing co-localization of Prox-1 GFP signal (green) and Itga-9 staining (red) on the luminal valve of the lymphatic vessel. Scale bars: 25μm.

3.1.1.3. Time course evaluation on pharmaceutical intervention on inflammatory lymphangiogenesis

To demonstrate the application of this mouse model for longitudinal investigation on LG and the effect of a pharmaceutical intervention, we performed a time course study and assessed the blockade effect of vascular endothelial growth factor receptor-2 (VEGFR-2) on inflammatory LG induced by suture placement[82,84]. As shown in Fig 5a, a systemic blockade via intraperitoneal injection of VEGFR-2 neutralizing antibodies led to a significant suppression of inflammatory LG in the cornea. Summarized data from repetitive experiments are presented in Fig 5b.

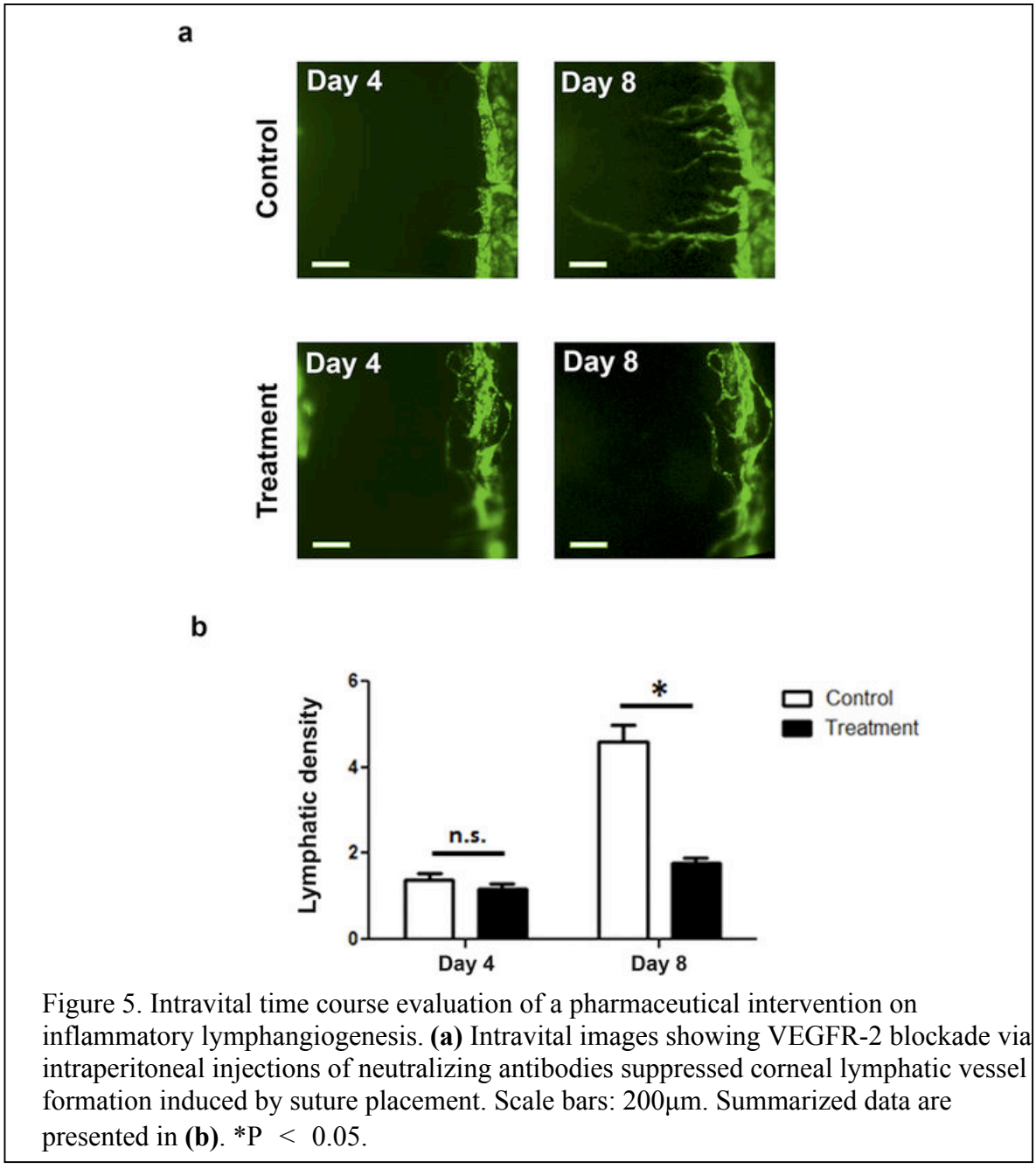

Figure 5. Intravital time course evaluation of a pharmaceutical intervention on inflammatory lymphangiogenesis. **(a)** Intravital images showing VEGFR-2 blockade via intraperitoneal injections of neutralizing antibodies suppressed corneal lymphatic vessel formation induced by suture placement. Scale bars: 200μm. Summarized data are presented in **(b)**. *P $<$ 0.05.

3.1.1.4. Lymphatic valvulogenesis is initiated inside the limbal vessels

We next explored more details on the dynamics of the lymphangiogeneic event using the transplantation model, which vigorously induced both LG and VG, compared to other models (Fig 3 and 6). Surprisingly and interestingly, we found that VG was first initiated inside pre-existing limbal vessels after lymphatic sprouts budded from them. As shown in Fig 6a, while only one valve was observed forming inside the limbal vessel on 8 days post transplantation, two more valves were detected within 3 days.

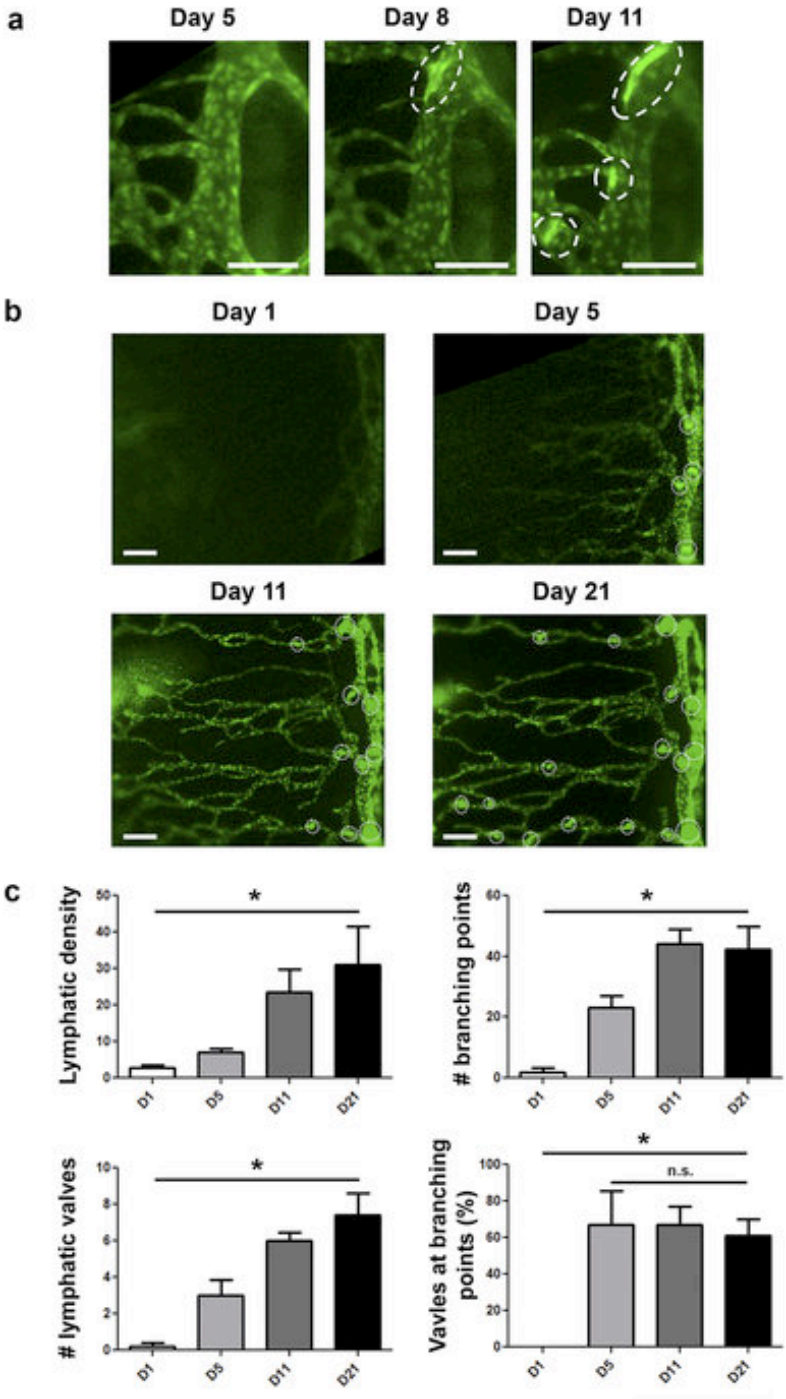

Figure 6. Intravital time course imaging showing the initiative and progressive processes of lymphangiogenesis and valvulogenesis after transplantation. **(a)** Intravital time course evaluation on the initiation and progression of valve formation within limbal vessels. Scale bars: 100μm. **(b)** Intravital time course evaluation on progressive lymphangiogenesis in parallel with valvulogenesis into central cornea after transplantation. Scale bars: 150μm. Vertical vessel to the right of the panel: limbal vessel; Dotted circles: newly formed valves. **(c)** Summarized data showing time course increase of lymphatic density, branching points, and valves. Lymphatic valves are predominantly located at the branching points across the time points studied with progressive LG and VG. *P $<$ 0.05.

3.1.1.5. Progressive valvulogenesis along with advancing lymphangiogenesis into central cornea

Following limbal vessel valve formation and along with LG marching into the central cornea, more valves were formed inside the elongating lymphatic vessels in time course (Fig. 6b). In the first week post transplantation, lymphatic sprouts were detected budding from limbal vessels indicating the early stage of LG. As the vessels advanced into the central cornea in the following 2 weeks, an increasing number of valves were observed inside these vessels as they extended. Summarized data reflecting the time course increases of lymphatic vessels and valves are presented in Fig 6c. Moreover, we have also assessed the relationship between branching points and the location of lymphatic valves and found that across the time studied with progressive LG and VG, lymphatic valves were predominantly located near the branching points (Fig. 6c), and this result is in consistent with our previous one time point ex vivo study in the suture model[18].

3.1.1.6. Lymphatic endothelial stalk cell migration during vessel elongation

Excitingly, with the live imaging technique, we were also able to divulge another important phenomenon and mechanism underlying lymphatic elongation, which is endothelial stalk cell lateral migration. As shown in Fig 7, within a short period of 2 minutes, two stalk cells in close proximity had departed along the axis of vessel extension. This dynamic event occurring in the middle of a lymphatic branch is more vividly presented in Supplementary Video 1.

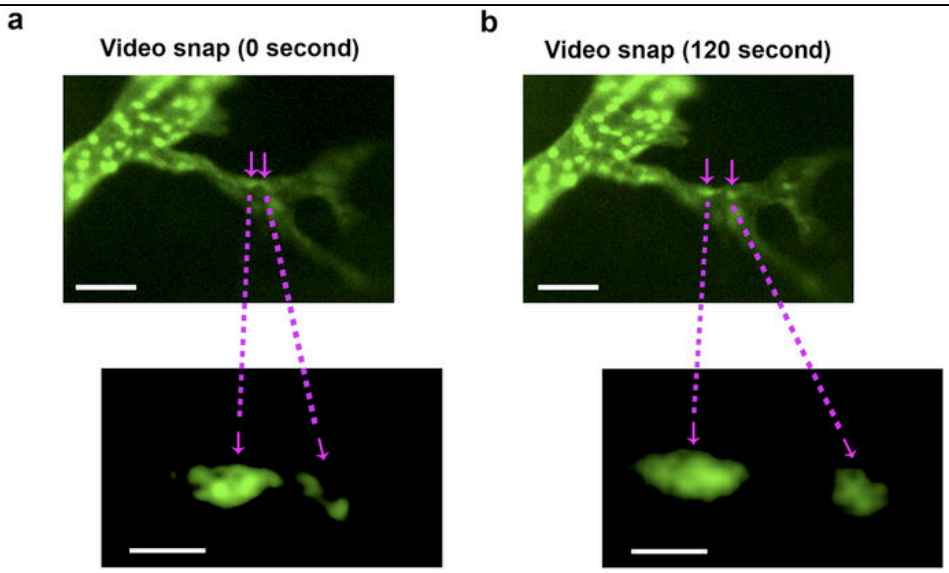

Figure 7. Intravital video showing lateral migration of stalk cells during lymphatic elongation. Snap pictures of intravital video illustrating departure of two endothelial stalk cells (indicated by magenta arrows) along the axis of vessel elongation. (**a,b**, top panels) Images showing the close proximity of the two cells before separation (**a**, 0 second) and after lateral migration (**b**, 120 seconds). Scale bars: 25μm. Corresponding magnified images are presented in the lower panels. Scale bars: 5μm.

3.1.1.7. Lymphatic pruning at early phase of lymphangiogenesis

During the early phase of LG and within 3 weeks after transplantation, we also detected another novel phenomenon of lymphatic pruning. This appeared as a retraction of lymphatic fronts or tips of newly forming lymphatic capillaries while the other vessels were still growing and elongating (Fig. 8a).

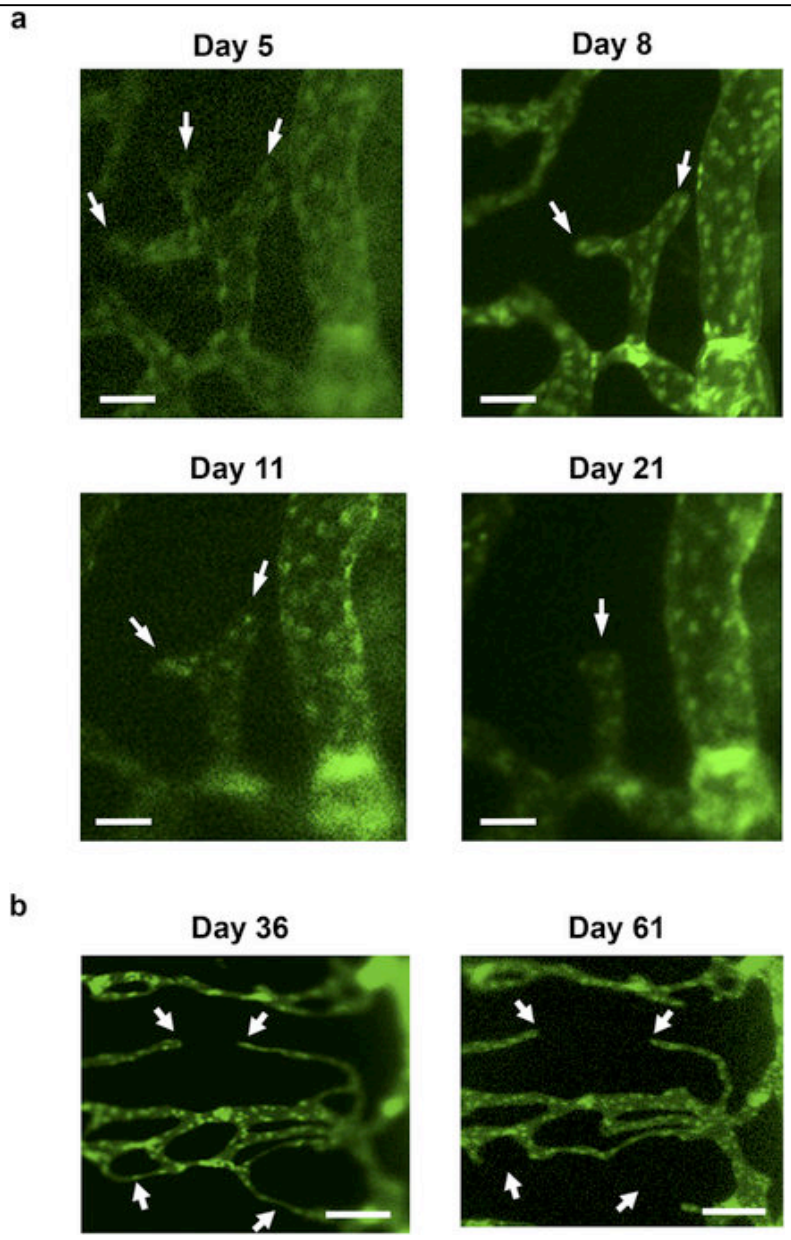

Figure 8. Intravital time course imaging demonstrating processes of lymphatic pruning and regression at the early and late stages after transplantation. **(a)** Representative intravital images showing a pruning process by tip retraction. Arrow: tip of lymphatic vessel. Scale bars: 50μm. **(b)** Representative intravital images illustrating a regression process by breakage in the middle of the lymphatic branches. Arrow: site of breakage. Scale bars: 150μm.

3.1.1.8. Lymphatic regression at late stage of lymphangiogenesis

In contrast, at the late stage of LG and after the lymphatic vessels reached to their maximal length around 3 weeks post transplantation, the process of lymphatic regression was observed with breakages in the middle of lymphatic branches, as illustrated in Fig 8b.

3.1.2. Discussion

In summary, this study using intravital imaging reveals novel aspects of the lymphangiogeneic events on both LG and VG in the cornea, one of the most favorite tissues for lymphatic research. These include progressive LG budding from the limbal vessels and marching into the central cornea, and subsequent valve formation and dissemination into the elongating lymphatic vessels after transplantation. In addition, we have divulged several novel phenomena involved in these dynamic events, such as the initiation of VG from inside limbal vessels, the spatial and temporal relationship between LG, lymphatic branching formation and VG, and distinctive patterns of lymphatic vessel elongation, pruning, and regression at different stages. We have exhibited as well the possibilities of using the live imaging model to examine blood vessels in parallel to lymphatic vessels and to evaluate the therapeutic effect of a pharmacological intervention.

Intravital imaging has great advantages over conventional immunohistochemical method with dead tissues[82]. Without live imaging, it is impossible to track the dynamic changes of LG/VG in the same tissue or subject for a period of time and at the physiological status. This technical limitation has created enormous knowledge gaps in our understanding of the real processes engaged in pathological lymphangiogeneic events. In this study with the live imaging system, we have been able to track the same tissue and site over a short or long period of time and have obtained the first evidence revealing the dynamics of LG and VG induced by transplantation. The high quality intravital images and videos acquired over the course allow us to perform detailed temporal and spatial analysis on the vessels and valves at their natural status and this in-depth analysis leads to the discovery of several new and important phenomena that cannot be detected with conventional ex vivo methods.

Our finding that in the setting of pathological LG in adult mammalian tissue, lymphatic elongation is achieved by lateral migration of the stalk cells is both novel and important. It offers the first, direct, in vivo and in real time evidence on a critical cellular mechanism underlying pathological LG, which merits further investigation. It is speculated that lymphatic pruning may facilitate more efficient lymphatic flow by reducing the number of overall branches, similar to synaptic pruning[88], which is yet to be explored. Our finding that lymphatic valves are first formed inside the pre-existing limbal vessels indicates that the limbal vessels not only give rise to lymphatic sprouts but also equip themselves with more valves for increased lymph flow in the diseased tissue. Collectively, pruning and valve formation may contribute to lymphatic maturation leaving functional vessels in network.

Research on corneal transplantation and LG is important because LG accompanies many diseases after inflammatory, chemical, infectious, immunogenic, or traumatic damage[16], and it is a primary mediator of corneal transplant rejection[29,30]. LG-invaded corneas are hostile to transplants for vision restoration due to a high rejection rate reaching 50–90%, irrespective of current treatment modality[16,23,26]. It is thus crucial to investigate the dynamics of LG and to obtain real time information on when and how LG is initiated, progressed, remodeled, and regressed, which are prerequisites for developing new and effective therapeutic approaches for corneal graft rejection in the future.

Furthermore, corneal LG research has broader implications beyond the eye. The cornea has been used by many scientists in broad fields to investigate neo-vascular events for decades. It has been employed for tumor angiogenesis research since 1970s[89] and more recently for LG research since 1990s[16,87]. Results from corneal vascular studies have also been proven to be readily applicable to other sites of the body. While a study using the corneal transplantation model has provided the first evidence on the importance of the lymphatic pathway in mediating graft rejection[43], this concept has later been corroborated in other major organ transplantations as well[15,61,90-92]. Since the lymphatic network penetrates most tissues in the body and pathological LG has been associated with a wide array of disorders including cancer metastasis, and inflammatory and immune diseases[15,17], it is plausible to predict that the lymphatic changes we observe in the cornea, whether in a short or long period of time, may also occur in other sites of the body. Results from this study may shed some light on our understanding and management of other LG-related disorders as well.

Taken together, we anticipate this study will facilitate lymphatic research in broad fields. Future investigation using the intravital imaging and on the novel phenomena promises for filling our knowledge gaps in understanding pathologic LG with VG and their management at various stages and inside or outside the eye.

3.2. ROLE OF LYMPHANGIOGENESIS AND VALVULOGENESIS ON CORNEAL TRANSPLANT REJECTION

3.2.1. Integrin alpha 9 blockade suppresses lymphatic valve formation and promotes low-risk graft survival

From: Kang, G. J., Truong, T., Huang, E., Su, V., Ge, S., & Chen, L. Integrin Alpha 9 Blockade Suppresses Lymphatic Valve Formation and Promotes Transplant Survival. Investigative Opthalmology & Visual Science, (2016).

3.2.1.1. Results

3.2.1.1.1. Effect of Itga-9 Blockade on Lymphatic Valvulogenesis After Corneal Transplantation

We first studied the effect of Itga-9 blockade on corneal LG and VG induced by transplantation. Either Itga-9 neutralizing body or isotype control was injected subconjunctivally twice a week starting from the surgery date. As demonstrated in Fig 9A, following the treatment with the Itga-9 blocking antibody, corneal lymphatic vessels contained significantly fewer valves compared with the control condition. Summarized data from repetitive experiments are presented in Fig 9B (left; $P < 0.05$). However, this treatment had no effect on LG, as shown in Fig 9B (right). Our further analysis on the ratio of valve quantity to lymphatic invasion area revealed a significant reduction in this parameter in the treated rather than the control condition (Fig.9C; $P < 0.05$).

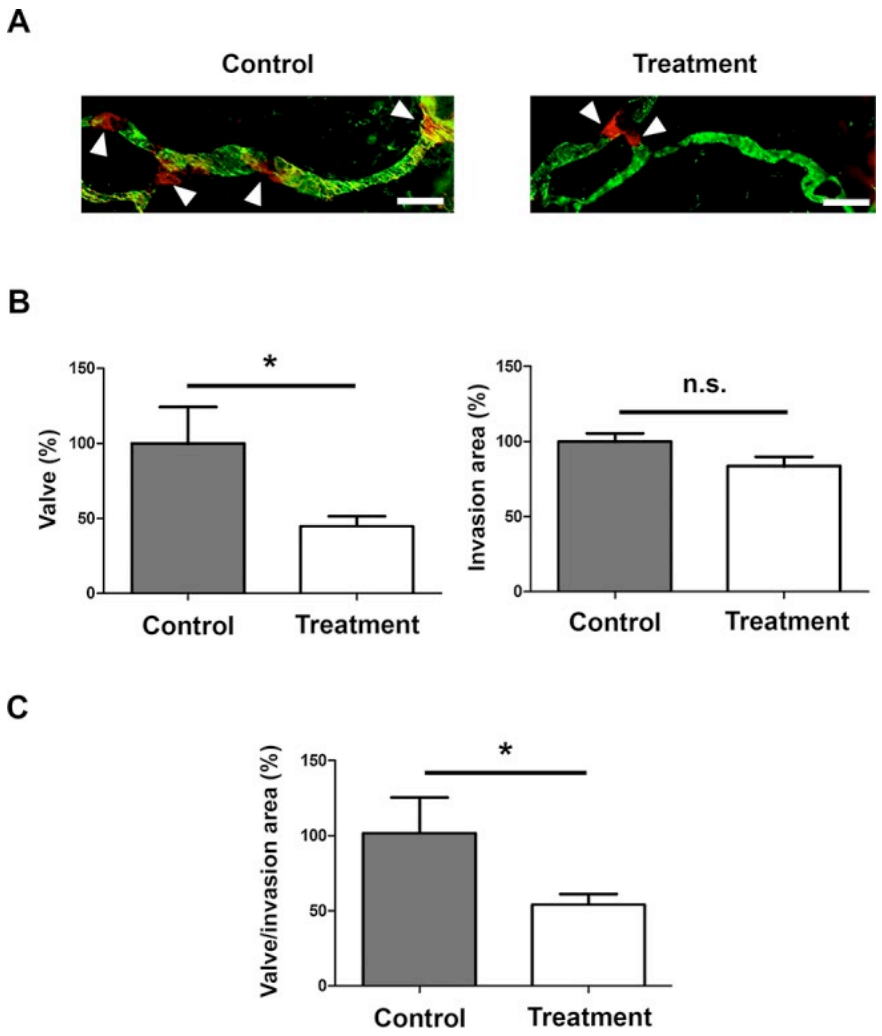

Figure 9. Lymphatic VG was suppressed by Itga-9 blockade after corneal transplantation. **(A)** Representative whole-mount immunostaining images demonstrating significantly fewer valves in the Itga-9 blocking antibody–treated cornea in comparison with isotype control–treated cornea. Red: Itga-9; Green: LYVE-1. Scale bars: 100μm. **(B)** Comparative quantification on lymphatic valves and lymphatic vessel invasion area in control and treatment conditions. Anti–Itga-9 treatment only reduced valve formation. The experiment was repeated twice with seven mice in control and eight mice in treatment group. *$P < 0.05$; n.s., not significant. **(C)** Comparative quantification showing significant lower ratio of valves to lymphatic invasion area in response to anti–Itga-9 treatment. The experiment was repeated twice with seven mice in control and eight mice in treatment group. *$P < 0.05$.

3.2.1.1.2. Effect of Itga-9 Blockade on Nasal Dominant Distribution of Lymphatic Vessels

Previously, we reported that corneal lymphatic vessels observe a unique nasal dominant distribution pattern in inflammatory LG[19,93]. To investigate whether this phenomenon also manifests in transplantation-associated LG and whether it is affected by the Itga-9 treatment, I next investigated the effect of Itga-9 blockade on the polarity of LG by comparing the nasal and temporal quadrants, as illustrated in Fig 10A. Our results showed that in both treatment and control groups, lymphatic vessels were more distributed at the nasal side, and Itga-9 blockade had no effect on this polarity of corneal LG (Fig.10B and 11). Our further association analysis using the linear mixed model also confirmed that the polarized distribution of LG was associated only with corneal regions but not with the anti–Itga-9 blockade.

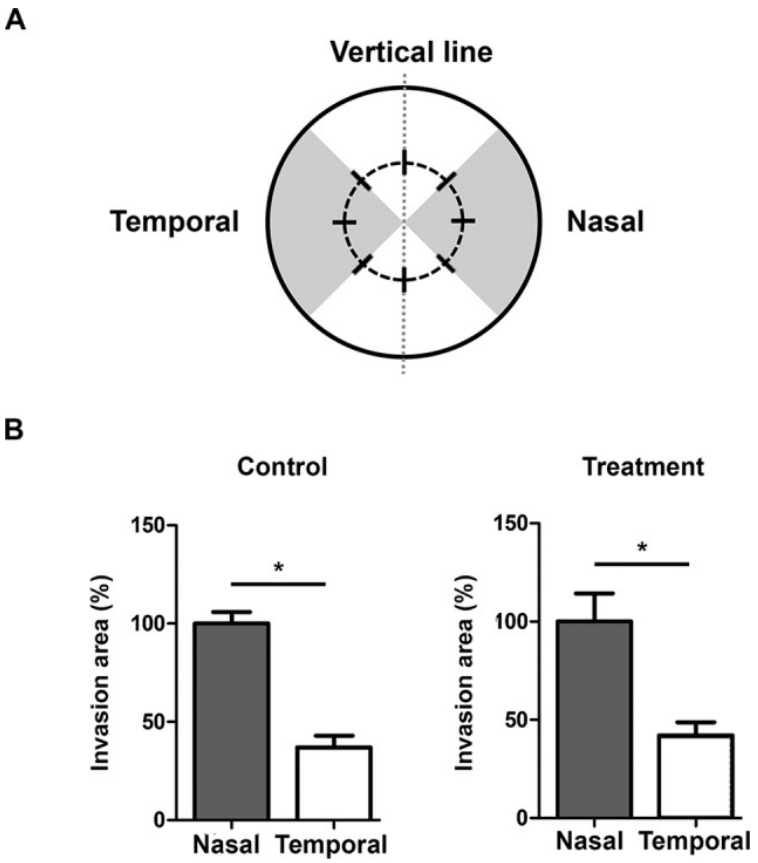

Figure 10. Itga-9 blockade had no effect on polarized distribution of lymphatic vessels after corneal transplantation. **(A)** Schematic illustration of nasal and temporal quadrant areas used for quantification. Eight short lines around the clock indicate sutures placed along the graft border. Outer solid circle: limbus. Inner dotted circle: graft border. Vertical line: separation between the nasal and temporal sides. Gray-shaded regions: nasal and temporal areas evaluated. **(B)** Comparative quantification showing significantly greater lymphatic invasion area in the nasal rather than the temporal side in both control and treatment conditions. The experiment was repeated twice with seven mice in control and eight mice in treatment group. *$P < 0.05$.

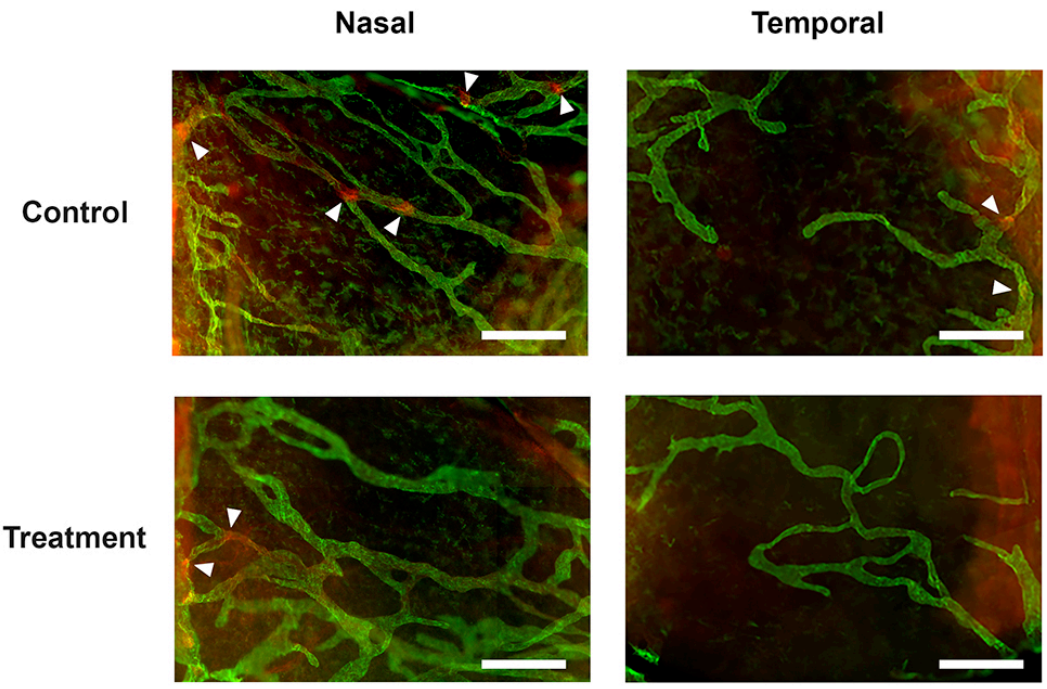

Figure 11. Representative immunofluorescent microscopic images showing lymphatic vessels and valves in the corneas eight weeks after transplantation. Arrow heads: lymphatic valves. Red: Itga-9; Green: LYVE-1. Scale bars: 200μm.

3.2.1.1.3. Effect of Itga-9 Blockade on Corneal Graft Survival

To further evaluate the effect of Itga-9 blockade on corneal graft survival, I examined the grafts in both treatment and control groups and evaluated their survival rate twice a week up to 8 weeks after the surgery. As shown in Fig 12, our results showed a significant promotion of graft survival by this treatment. Although graft rejection in both the control and treatment groups started approximately 2.5 weeks after transplantation, a significantly higher percentage of the grafts survived in the treatment group by the end of the 8-week study, as analyzed by the Kaplan-Meier survival curves ($P < 0.05$).

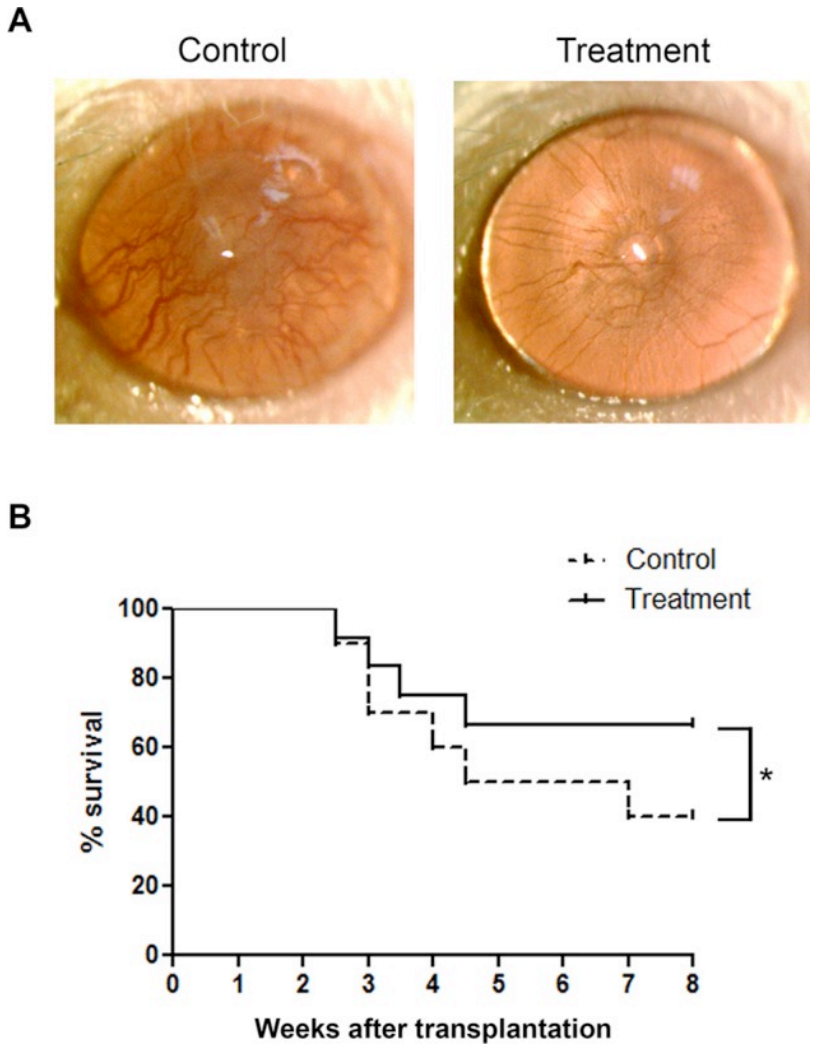

Figure 12. Itga-9 blockade promoted corneal graft survival. **(A)** Representative images from slit-lamp examination of rejected and survived grafts in control and treatment conditions, respectively. **(B)** Kaplan-Meier survival curves showing significantly higher survival rate in the treatment group. *P < 0.05.

3.2.1.2. Discussion

In this study, we demonstrated for the first time that Itga-9 is critically involved in corneal transplantation–induced VG, and its molecular blockade can effectively suppress this process. We have also shown that this treatment strategy does not affect corneal LG or its polarity of nasal distribution. More importantly, we have offered the first evidence showing that by reducing the lymphatic valves but not the vessels themselves, we were able to achieve a higher rate of graft survival.

Our finding that Itga-9 blockade suppressed lymphatic valve formation without disturbing the lymphatic vessels in transplantation is consistent with our previous report

on a suture-induced inflammation model[46]. It seems that lymphatic valves are more responsive to Itga-9 intervention than lymphatic vessels. This may be explained by the fact that Itga-9 is more highly expressed on the valves than the vessel walls, as shown in Fig 13 with a transplanted cornea. The disparity between lymphatic valves and vessels was also observed during development, in which a reduced number of lymphatic valves, but not vessels, were detected in Itga-9 knockout mice[94]. With the treatment regimen used in this study, we did not observe any obvious side effects. For future development of clinical application, it may be possible to achieve the therapeutic effects by using various formats of the antagonists against the Itga-9 pathway, such as neutralizing antibodies or small molecules, which merits further investigation and is beyond the scope of this report.

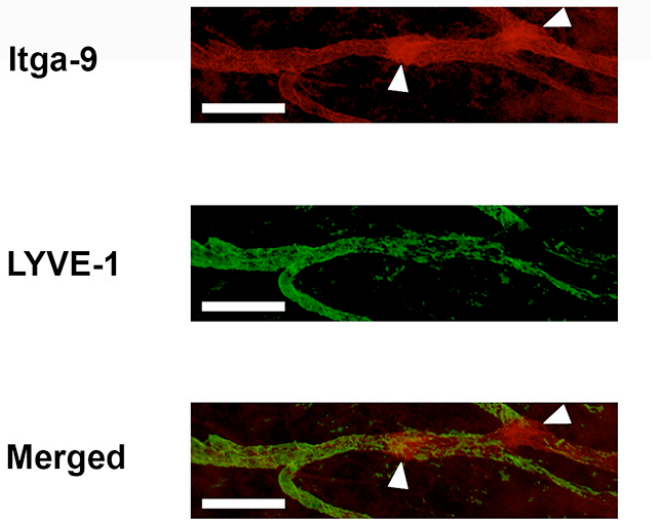

Figure 13. Representative immunofluorescent microscopic images showing higher expression of Itga-9 on lymphatic valves than vessel walls in the grafted cornea. Arrow heads: lymphatic valves. Red: Itga-9; Green: LYVE-1. Scale bars: 100μm.

It is remarkable that prevention of lymphatic valve formation can significantly increase graft survival. This finding indicates a compromise of the immune reflex arc in which the lymphatic pathway serves as the afferent arm[16,26]. It also aligns well with a previous developmental report that Itga-9 knockout mice died shortly after birth from bilateral chylothorax, in which lymphatic vessels were present but displayed compromised integrity[95]. Moreover, our lab has reported that lymphatic vessels are equipped with valves as they become mature and functional[19]. Therefore, by targeting on lymphatic valves, we may have interfered with the maturation process of the lymphatic vessels, rendering them dysfunctional. It would be interesting to check if this strategy also affects other indices of the immune responses involved in transplant rejection, such as delayed-type hypersensitivity, which warrants further investigation.

In summary, this study reveals an important role of lymphatic VG in mediating transplant rejection. It also provides a novel therapeutic strategy to effectively interfere with this pathological process and to improve graft survival. As one of the favorite tools for lymphatic study in general, our results from the cornea may shed some light on the development of new Itga-9–based therapies to treat broader lymphatic and immune diseases in the body.

3.2.2. Combined blockade of VEGFR-3 and Itga-9 inhibits corneal lymphangiogenesis and valvulogenesis *in vivo* and promotes high-risk graft survival

3.2.2.1. Results

3.2.2.1.1. Effect of combined blockade of VEGFR-3 and Itga-9 on LG after high-risk corneal transplantation

I first evaluated if LG was effectively blocked by combined treatment after high-risk corneal transplantation from BALB/c donor to fully mismatched Prox-1 GFP C57Bl/6 recipient mice with intravital images obtained in time course. Representative images clearly demonstrated that treated corneas had no LG whereas control corneas have shown robust LG that pertained to late stage (Fig. 14).

I then quantified the level of LG in recipient bed and donor button of each individual cornea to compare between control and treated groups based on intravital images as described previously (Fig. 15A). Treated group had absolutely no LG both in the recipient and donor area showing significant difference from control condition (Fig. 15B; $p < 0.05$). It was notable that control group in recipient bed sharply inclined at 1 week and reached the peak at 2 weeks post transplantation where treated group has shown no progression of all time. In donor buttons, control group started increasing from week 2 when recipient bed reached almost the peak and kept increasing until week 3 where LG already reached the peak in recipient bed. While host bed of control group maintained the full level of lymphatic vessel invasion since week 3, invasion area in donor corneal area slightly decreased over time.

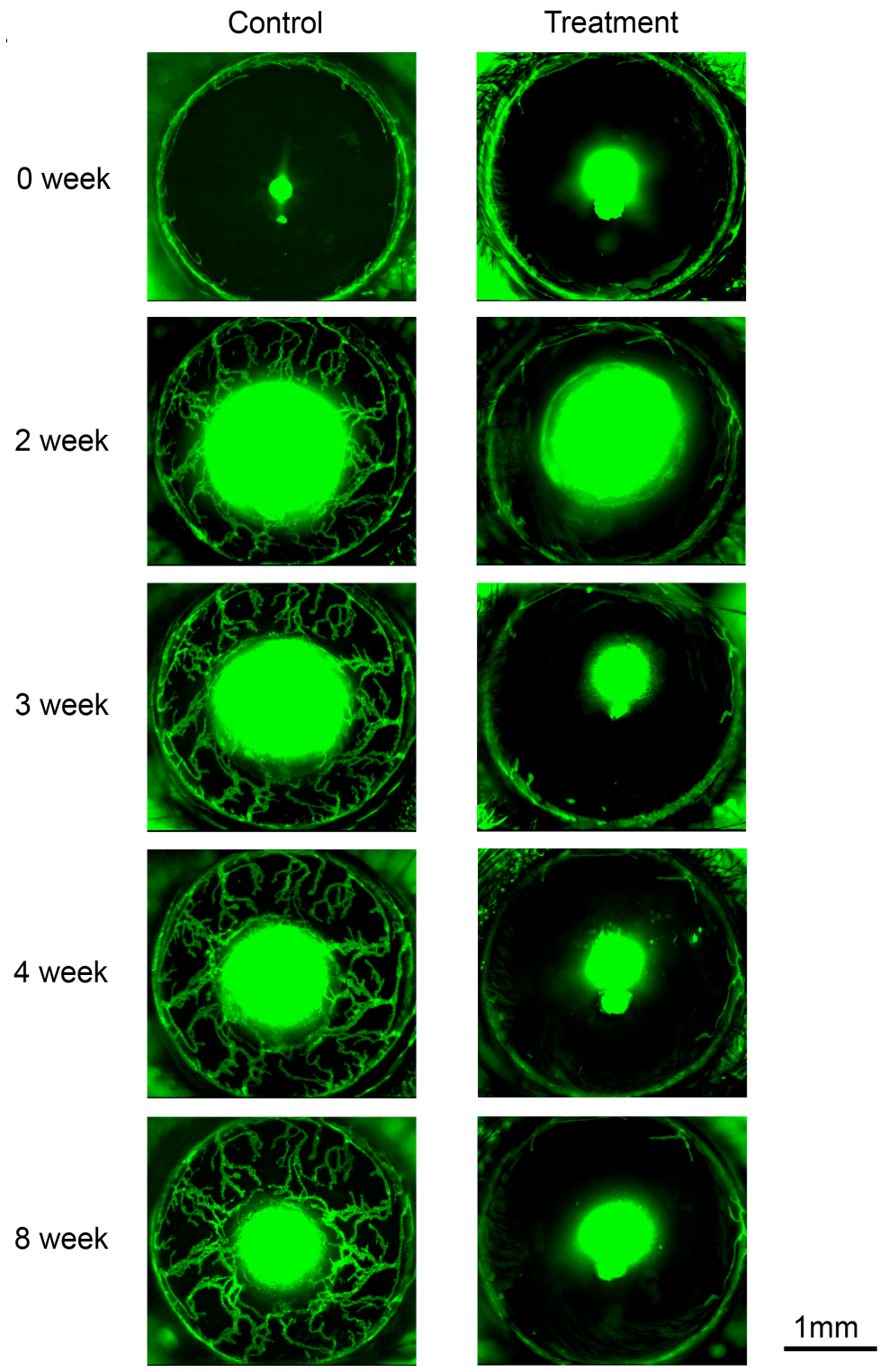

Figure 14. Representative intravital time course images in control and treated cornea after high-risk corneal transplantation. Combined blockade suppressed lymphangiogenesis after corneal transplantation. Scale bar: 1 mm.

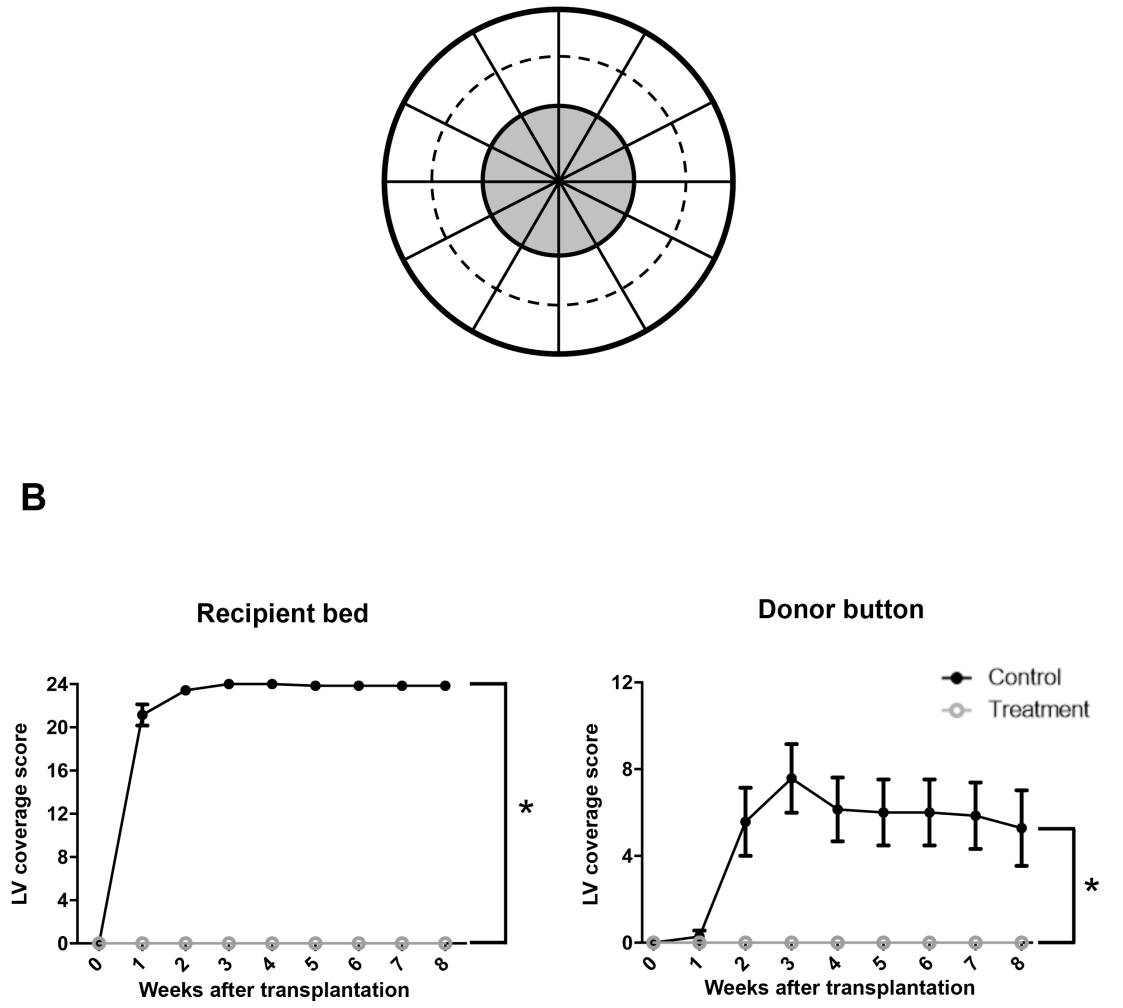

Figure 15. Combined treatment completely blocked lymphangiogenesis. (A) Schematic illustration of donor and recipient areas used for lymphangiogenesis quantification. Outer solid circle: limbus. Inner solid circle: donor-recipient boundary. Lines around the clock and dashed circle: dividing lines for each sector to be counted. (B) Comparison of lymphatic vessel invasion area between control and treated corneas in recipient beds and donor buttons. * P<0.05. Error bars represent ±SEM (n=7 in control, n=8 in treatment).

3.2.2.1.2. Effect of combined blockade of VEGFR-3 and Itga-9 on VG after high-risk corneal transplantation

I also quantified the number of newly formed valves in each cornea to compare between control and treated groups (Fig. 16A). Fig. 16B demonstrates a representative image of the lymphatic valve detected by intravital imaging. Control group exhibited vigorous VG at 1 and 2 weeks post transplantation and kept the high number of valves until 8 weeks

whereas treated group demonstrated a small peak at week 1 and continuous decline thereafter showing a significant difference from the control group (Fig. 16C; $p < 0.05$).

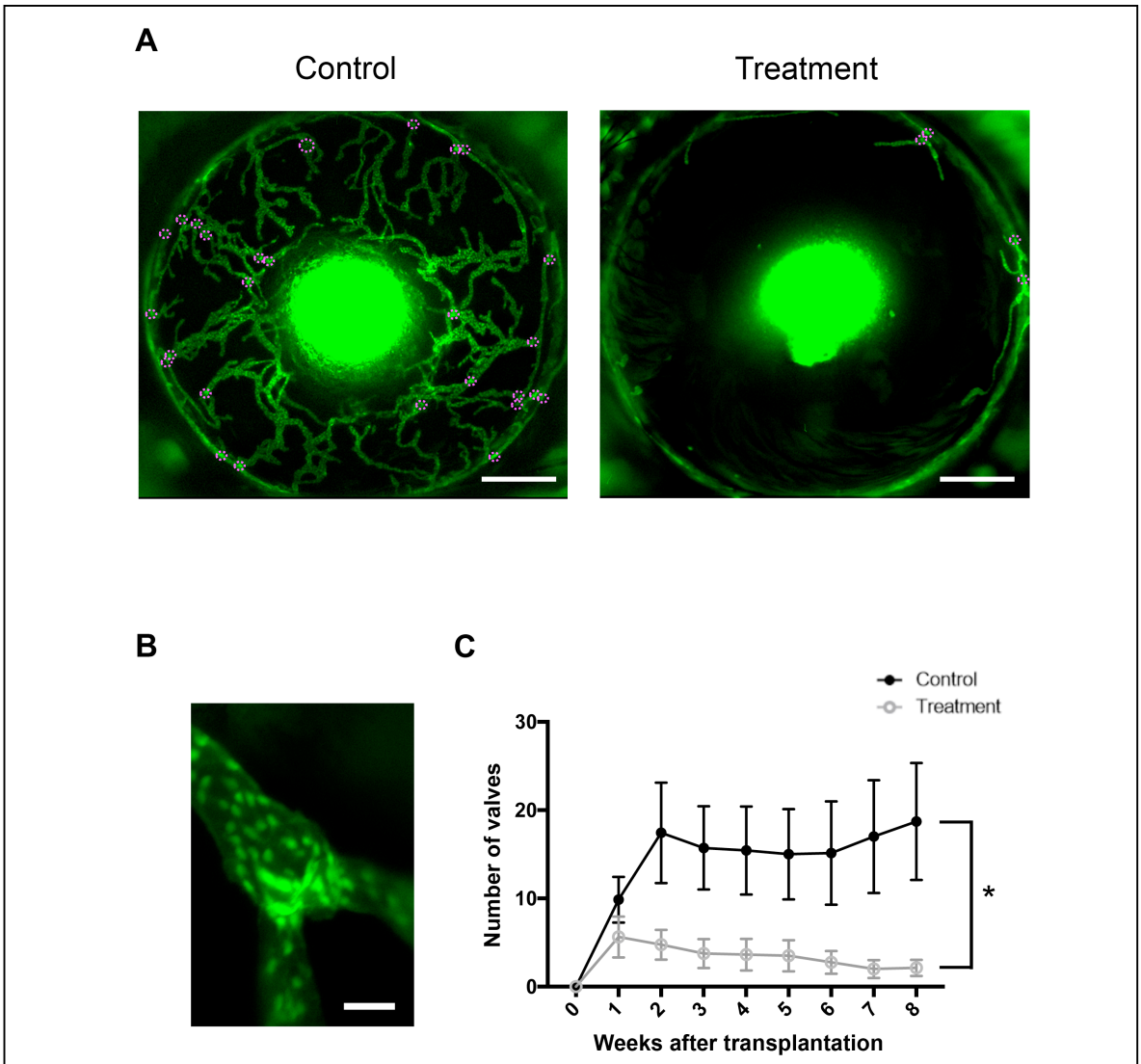

Figure 16. Combined treatment significantly suppressed valvulogenesis. (A) Representative intravital images of lymphatic valves in control and treated cornea at 8 weeks after transplantation. Dotted magenta circles: lymphatic valves. Scale bars: 500μm. (B) Representative intravital image of a lymphatic valve. Scale bar: 50μm. (C) Number of newly formed lymphatic valves in control and treated cornea over time. * P<0.05. Error bars represent ±SEM (n=7 in control, n=8 in treatment).

3.2.2.1.3. Effect of combined blockade of VEGFR-3 and Itga-9 on high-risk graft survival

Graft survival after high-risk transplantation was evaluated with slit-lamp observation of opacity scores. Fig. 17A illustrates representative slit-lamp images from a rejected graft

in the control group and an accepted graft in the treated group. Fig. 17B presents treated group had 40% increased survival rate at 8 weeks post transplantation in Kaplan-Meier survival curve.

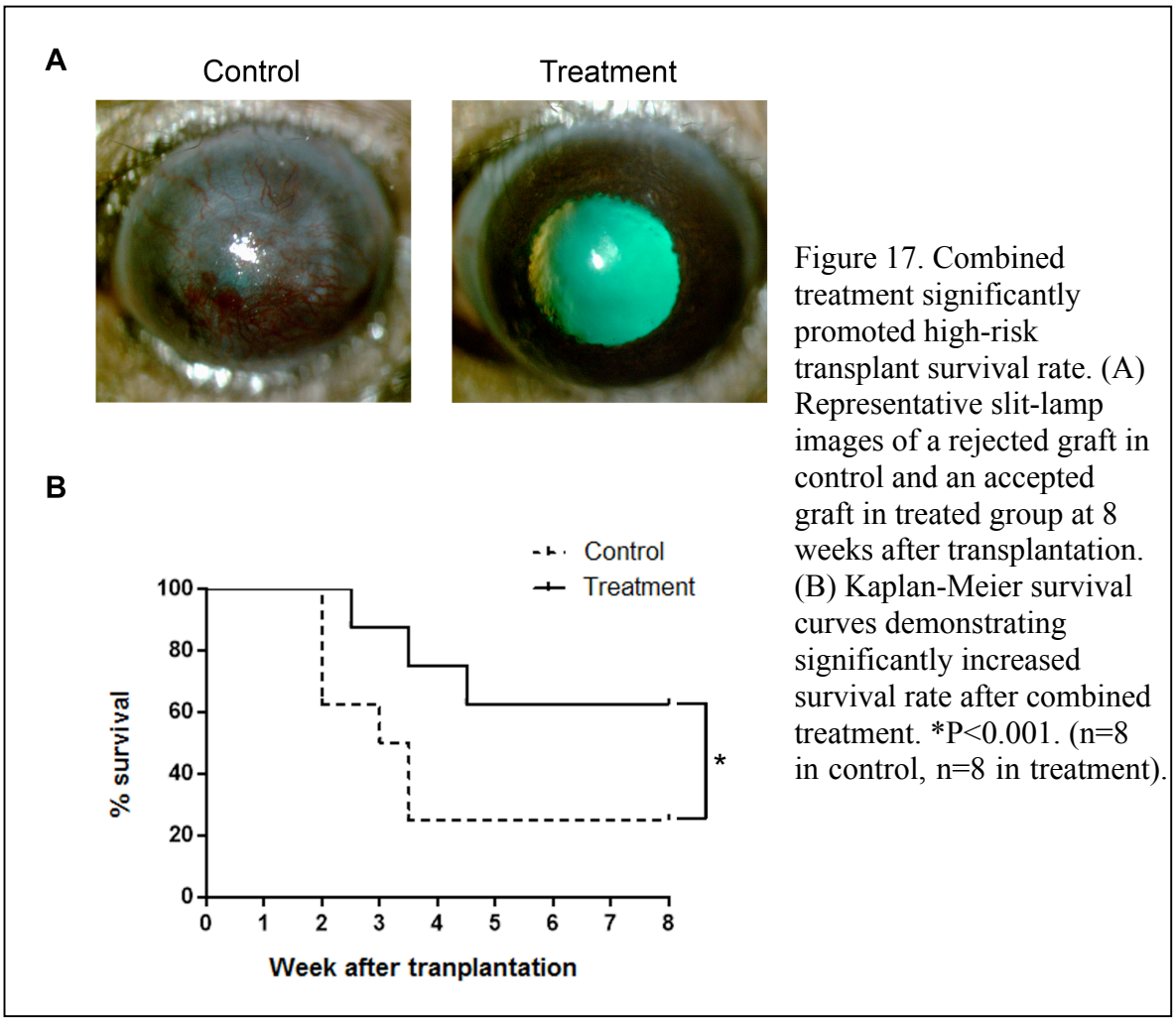

Figure 17. Combined treatment significantly promoted high-risk transplant survival rate. (A) Representative slit-lamp images of a rejected graft in control and an accepted graft in treated group at 8 weeks after transplantation. (B) Kaplan-Meier survival curves demonstrating significantly increased survival rate after combined treatment. *P<0.001. (n=8 in control, n=8 in treatment).

3.2.2.1.4. Effect of combined blockade of VEGFR-3 and Itga-9 on central corneal thickness

Anterior segment OCT was used to measure the central corneal thickness of control and treated corneas (Fig. 18A). Combined treatment significantly reduced central corneal thickness at 2 and 3 weeks post transplantation when compared to control group (Fig. 18B; $p < 0.05$). Additionally, rejected corneas showed significant thickening of the cornea than accepted corneas where there was less change in the time course (Figure 5C; $p < 0.0001$).

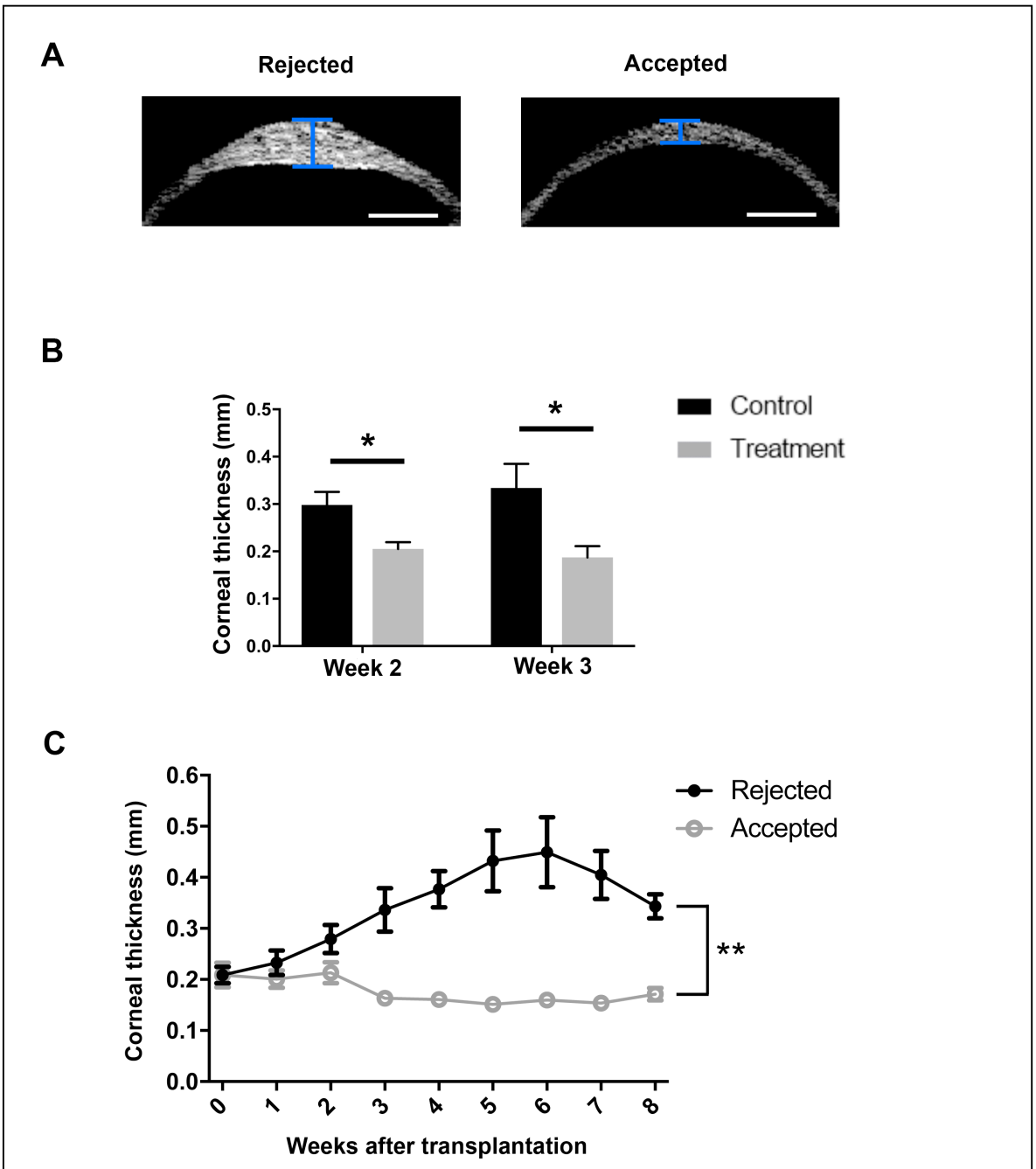

Figure 18. Combined treatment significantly decreased central corneal thickness. (A) Representative anterior segment OCT images showing rejected graft in control and accepted graft in the treated group at 8 weeks after transplantation. The survived graft demonstrated reduced thickness, as indicated by the blue brackets. Scale bar: 1mm. (B) Central corneal thickness was significantly reduced in treated than control group at 2 and 3 weeks after transplantation. * $P < 0.05$. Error bars represent ± SEM (n=8 in control, n=8 in treatment) (C) Central corneal thickening was significantly higher in rejected graft than in accepted ones. ** $P<0.0001$, Error bars represent ±SEM (n=7 in the accepted group, n=8 in the rejected group)

3.2.2.2. Discussion

In this study, we report combined blockade of VEGFR-3 and Itga-9 inhibited corneal LG and VG and significantly promoted high-risk transplant survival as well. Major findings of the current study are dynamic changes in LG and VG post surgery that was unseen before without intravital imaging. Combined treatment completely suppressed LG of all time by the end of this study. To our knowledge, there has been no report showing complete inhibition of LG after high-risk transplantation. Combined treatment against VEGFR-3 with other integrins, VLA-1 (also known as integrin α1β1) after high-risk transplantation was not able to block LG entirely either. This might be because blocking Itga-9 pathway synergized with VEGFR-3 treatment on LG. Though Itga-9 single treatment in vivo had no significant effect on LG, our in vitro data demonstrated that Itga-9 depletion in lymphatic endothelial cells (LECs) suppressed proliferation, adhesion, migration, and tube formation without affecting the viability of the cells implying that Itga-9 could have altered function of LECs37. Chen and his colleagues also suggested integrins crosstalk with VEGF-C/VEGFR-3 pathway via galectin-8[96].

Combined treatment has shown a synergistic effect on VG as well preventing most VG at 8 weeks post high-risk transplantation while Itga-9 single treatment suppressed about 50% of VG in low-risk transplantation[97]. In this study, VG in control group after transplantation peaked at week 2 whereas, our other report with suture placement model, it peaked at week 6. This might be because transplantation induces a vigorous immune response against donor tissue in early stage demanding highly active transport of cells and lymph fluids through lymphatic vessels unlike inflammatory response induced by suture placement only.

Our high-risk transplantation model utilizes histocompatibility fully mismatched mouse strains. Only 15–20% of BALB/c corneal grafts survive in C57BL/6 hosts, but with combined treatment of VEGFR-3 and Itga-9, transplant survival has promoted to 60% Further investigation is required to determine the effect of this treatment on high-risk transplantation. A worthy question to determine will be investigating the effect of this treatment in the middle or late stage of rejection. So far, combined treatment of VEGFR-2 and VEGFR-3 on inflammatory LG induced by suture placement could inhibit early and middle stages of LG, but not in late stage[84]. Many cases in the clinic, however, suffer from corneal transplant failure in host corneas with late stage LG which is in need of future efforts to develop new therapies.

In summary, this study provides new insights into the dynamic changes of LG, VG, and central corneal thickness during high-risk transplant rejection. It also reveals combined treatment of VEGFR-3 and itga-9 significantly promotes high-risk corneal transplant survival via total suppression of LG and significant reduction of VG. This method may pave the way for a novel therapeutic strategy to interfere pathological processes not only involved in transplant rejection, but also other lymphatic- and immune-related diseases in the body.

3.3. CELLULAR ORIGIN OF CORNEAL LYMPHANGIOGENESIS

3.3.1. Results

To determine cellular origin of LECs in the cornea during inflammation other than pre-existing limbal lymphatic vessels, I investigated the contribution of corneal resident cells and BM derived cells. The uninflamed central cornea of Prox-1 GFP mouse was transplanted to Prox-1 tdTomato recipient to exclude any pre-existing LECs and followed by intravital imaging. No GFP+ cells were detected in tdTomato+ newly formed vessel network in the recipient mouse up to 120 days after transplantation (Fig. 19).

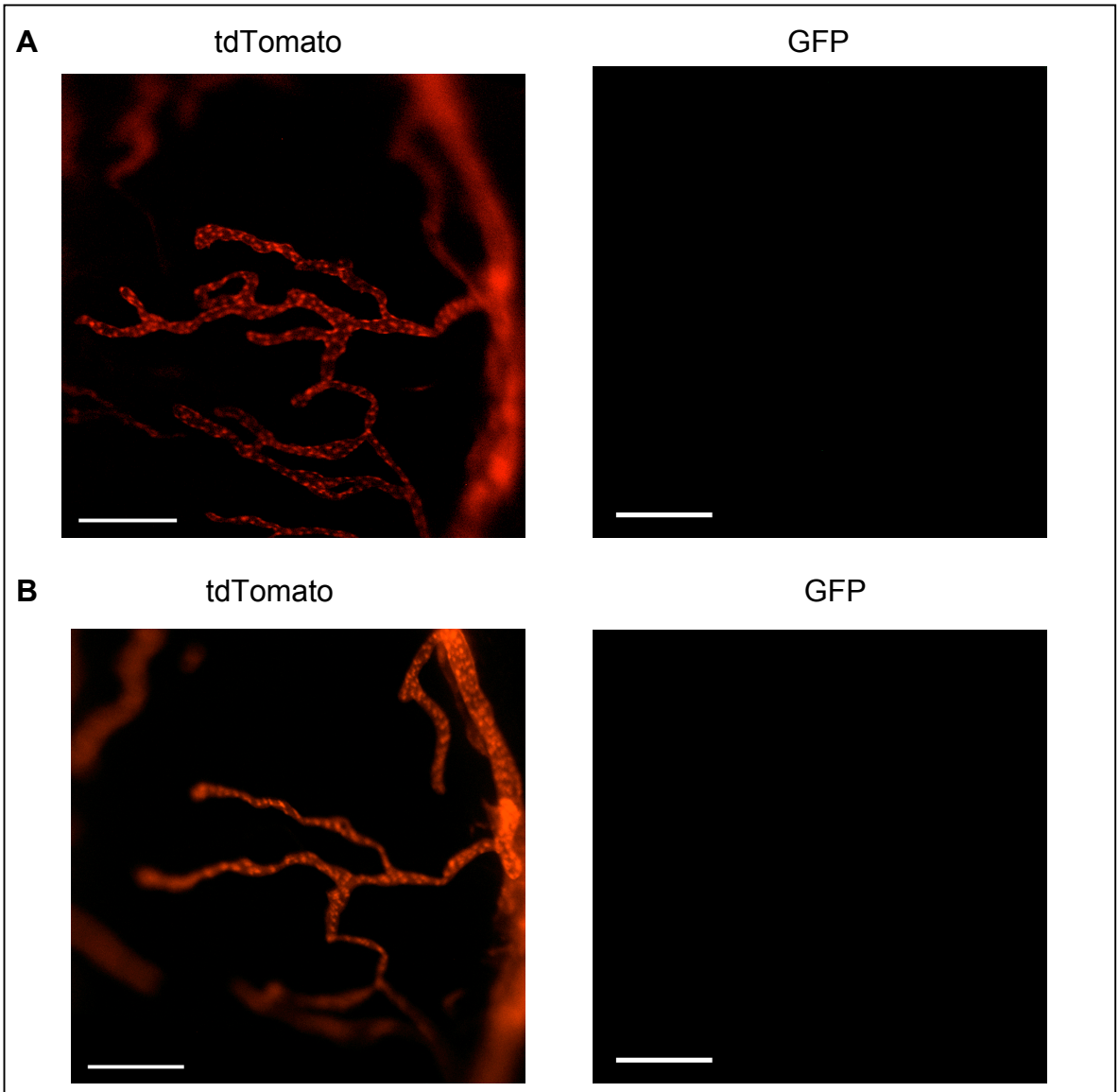

Figure 19. Representative intravital image of the same Prox-1 tdTomato transplant recipient cornea. No GFP+ donor corneal tissue derived cell was found in the newly formed lymphatic network. (A) 3 weeks post transplantation, Scale bars: 250µm. (B) 120 days post transplantation. Scale bars: 250µm.

To determine the contribution of BM derived cells in corneal LG, I performed BM transplantation from β-actin eGFP to C57BL/6 wild type mice or Prox-1 tdTomato mice. Successfully BM transplanted mouse corneas were sutured and carefully studied by intravital imaging and immunohistochemistry. eGFP+ cells with tdTomato+ nucleus were found in newly formed lymphatic vessels as early as 2 weeks post suture placement in Prox-1 tdTomato mouse as revealed by intravital imaging (Fig. 20A). The result was verified ex vivo by immunofluorescent microscopic assay using antibodies against LYVE-1 and Prox-1 at week 3, 11 and 15 after suture placement. GFP+ cells in the newly formed lymphatic vessels were found in all time points studied (Fig. 20B). The newly formed vessels were made up of a mosaic containing grafted BM derived cells and host endothelial cells. These data provide strong evidence for the contribution of BM derived cells in corneal LG.

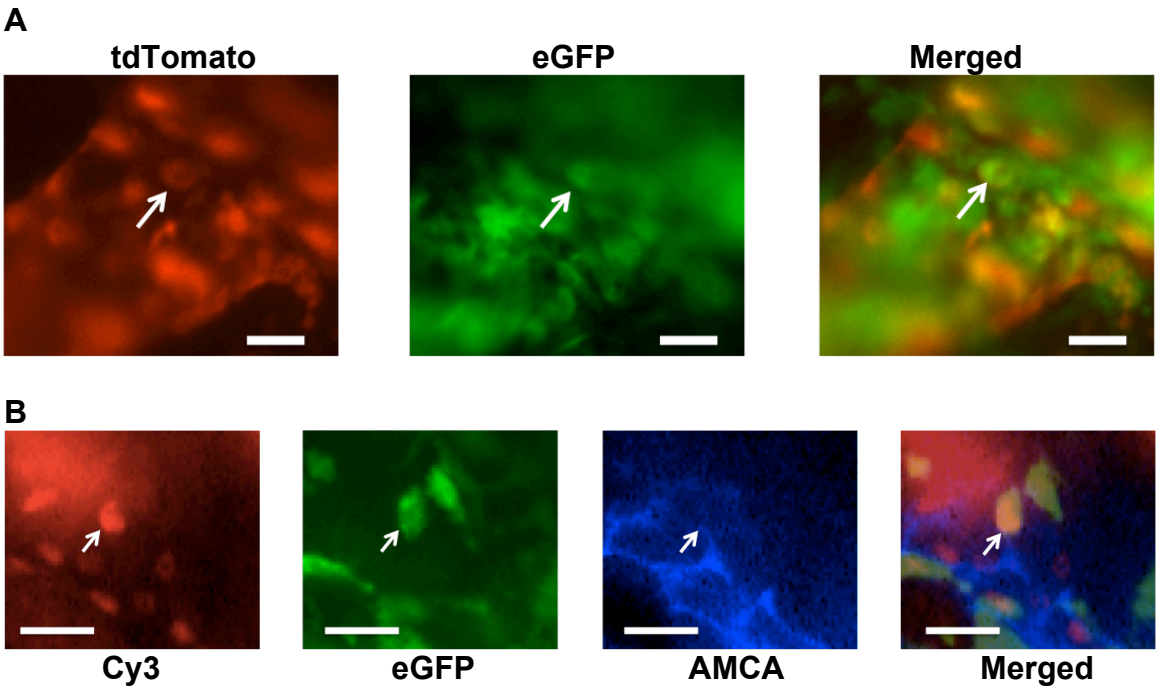

Figure 20. Representative images of BM derived cells in the newly formed lymphatic vessel. (A) Intravital image of Prox-1 tdTomato mouse cornea 2 weeks after suture placement. (tdTomato: Prox-1; eGFP: BM derived cells) Scale bars: 20μm. (B) Histochemical images of recipient mouse cornea 15 weeks after suture placement. (Cy3: Prox-1; eGFP: BM derived cells; AMCA: LYVE-1) Scale bars: 20μm.

3.3.2. Discussion

In these experiments, the lymphatics in the inflamed cornea are formed by a mosaic of grafted BM derived and host-derived LECs, not corneal resident cells. To my knowledge, this is the first *in vivo* evidence of BM derived cells integrating into newly formed lymphatic vessels during inflammation. This is consistent with previous findings showing BM derived cells contributing in corneal lymphangiogenesis[62,76]. Since the overwhelming

number of cells recruited during inflammation in the cornea after whole BM transplantation providing too much background, it can be improved by transplanting specified LEPCs from the bone marrow for further study.

In this model, we didn't find the contribution of donor corneal tissue derived Prox-1 GFP+ cells into corneal LG after transplantation, but this doesn't exclude all possibility of corneal tissue resident cells involved in corneal LG in the host bed. It might be because BM originated cells such as dendritic cells and macrophages resident in cornea tissue become vulnerable once isolated from the host body during the transplantation. It also needs further investigation by using inflamed donor cornea tissue in the future.

As described before, the mechanisms of lymphangiogenesis in adult recapitulate to a great extent that during embryo development. Our study indicates that lymphvasculogenic and lymphangiogenic mechanisms occur side by side in the inflamed cornea. It provides a crucial foundation for further studies of the roles of LEC biology and the development and maintenance of lymphatic vasculatures in health and disease.

4. SUMMARY

The present study has established novel findings of dynamic changes during corneal LG and VG revealed by the intravital imaging system. First, by tracing corneal LG and VG during inflammation in detail into cell level resolution, I was able to record numbers of exciting events, which has been unseen with traditional histochemical methods so far. Within the same tissue, I have shown progressive LG from the limbus toward the central cornea and following VG in the same manner. With longer observation over time, I also demonstrated lymphatic network rearrangement, pruning, in early LG and regression of old vessels. A deeper investigation also led me to find out longitudinal elongation of a vessel with two individual LECs departing from each other.

Next, I focused on the role of lymphatic valves in the newly formed corneal vessels in corneal transplant rejection. Lymphatic vessels serve as a highway to transport antigens and antigen presenting cells into draining lymph nodes leading to activation of immune cells and vigorous rejection reaction. Blocking lymphatic pathway to reduce corneal transplant rejection has shown promising results, but the role of lymphatic valves was unknown. Here, I demonstrated blocking VG via anti Itga-9 single treatment selectively reduced VG not LG and significantly increased survival rate after low-risk corneal transplantation. Moreover, I demonstrated that combined blockade of VEGFR-3 and itga-9 can show a synergistic effect on VG and LG and high-risk transplant survival. I used multiple in vivo imaging techniques including our newly developed intravital imaging system, OCT, and traditional slit-lamp microscopy to assess the results in details over the course post surgery. .

Lastly, I investigated the cellular origin of corneal LG to make the most of intravital imaging system and presented the first in vivo evidence of BM derived cells integrated into the newly formed corneal lymphatic vessel during inflammation.

In a nutshell, this study illustrates the molecular and cellular mechanisms of corneal LG and VG in various contexts revealed by cutting edge imaging techniques and a wide array of experimental models and approaches. The results from this study provide a foundation of further study which might lead to new therapeutic options for the treatment of lymphatic related diseases in the eye and throughout the body.

5. REFERENCES

1 DelMonte, D. W. & Kim, T. Anatomy and physiology of the cornea. *J Cataract Refract Surg* **37**, 588-598, doi:10.1016/j.jcrs.2010.12.037 (2011).

2 Fares, U., Otri, A. M., Al-Aqaba, M. A. & Dua, H. S. Correlation of central and peripheral corneal thickness in healthy corneas. *Cont Lens Anterior Eye* **35**, 39-45, doi:10.1016/j.clae.2011.07.004 (2012).

3 Forrester, J. V., Dick, A. D., McMenamin, P. G. & Roberts, F. *The Eye: Basic Sciences in Practice*. 3rd edn, (Saunders Ltd, 2007).

4 Dua, H. S., Gomes, J. A. & Singh, A. Corneal epithelial wound healing. *Br J Ophthalmol* **78**, 401-408 (1994).

5 Sridhar, M. S. Anatomy of cornea and ocular surface. *Indian J Ophthalmol* **66**, 190-194, doi:10.4103/ijo.IJO_646_17 (2018).

6 Boote, C., Dennis, S., Newton, R. H., Puri, H. & Meek, K. M. Collagen fibrils appear more closely packed in the prepupillary cornea: optical and biomechanical implications. *Invest Ophthalmol Vis Sci* **44**, 2941-2948 (2003).

7 Maurice, D. M. The transparency of the corneal stroma. *Vision Res* **10**, 107-108 (1970).

8 Meek, K. M. & Knupp, C. Corneal structure and transparency. *Prog Retin Eye Res* **49**, 1-16, doi:10.1016/j.preteyeres.2015.07.001 (2015).

9 Geroski, D. H., Matsuda, M., Yee, R. W. & Edelhauser, H. F. Pump function of the human corneal endothelium. Effects of age and cornea guttata. *Ophthalmology* **92**, 759-763 (1985).

10 Stiemke, M. M., Edelhauser, H. F. & Geroski, D. H. The developing corneal endothelium: correlation of morphology, hydration and Na/K ATPase pump site density. *Curr Eye Res* **10**, 145-156 (1991).

11 Azar, D. T. Corneal angiogenic privilege: angiogenic and antiangiogenic factors in corneal avascularity, vasculogenesis, and wound healing (an American Ophthalmological Society thesis). *Trans Am Ophthalmol Soc* **104**, 264-302 (2006).

12 Banerji, S. *et al.* LYVE-1, a new homologue of the CD44 glycoprotein, is a lymph-specific receptor for hyaluronan. *J Cell Biol* **144**, 789-801 (1999).

13 Wigle, J. T. & Oliver, G. Prox1 function is required for the development of the murine lymphatic system. *Cell* **98**, 769-778 (1999).

14 Kaipainen, A. *et al.* Expression of the fms-like tyrosine kinase 4 gene becomes restricted to lymphatic endothelium during development. *Proc Natl Acad Sci U S A* **92**, 3566-3570 (1995).

15 Alitalo, K. The lymphatic vasculature in disease. *Nat Med* **17**, 1371-1380, doi:10.1038/nm.2545 (2011).

16 Chen, L. Ocular lymphatics: state-of-the-art review. *Lymphology* **42**, 66-76 (2009).

17 Karaman, S. & Detmar, M. Mechanisms of lymphatic metastasis. *J Clin Invest* **124**, 922-928, doi:10.1172/JCI71606 (2014).

18 Truong, T., Altiok, E., Yuen, D., Ecoiffier, T. & Chen, L. Novel characterization of lymphatic valve formation during corneal inflammation. *PLoS One* **6**, e21918, doi:10.1371/journal.pone.0021918 (2011).
19 Truong, T., Huang, E., Yuen, D. & Chen, L. Corneal lymphatic valve formation in relation to lymphangiogenesis. *Invest Ophthalmol Vis Sci* **55**, 1876-1883, doi:10.1167/iovs.13-12251 (2014).
20 Bohigian, G. M. *et al.* Report of the organ transplant panel. Corneal transplantation. Council on Scientific Affairs. *JAMA* **259**, 719-722 (1988).
21 Foulks, G. N. & Sanfilippo, F. Beneficial effects of histocompatibility in high-risk corneal transplantation. *Am J Ophthalmol* **94**, 622-629 (1982).
22 Maguire, M. G. *et al.* Risk factors for corneal graft failure and rejection in the collaborative corneal transplantation studies. Collaborative Corneal Transplantation Studies Research Group. *Ophthalmology* **101**, 1536-1547 (1994).
23 Chong, E. M. & Dana, M. R. Graft failure IV. Immunologic mechanisms of corneal transplant rejection. *Int Ophthalmol* **28**, 209-222, doi:10.1007/s10792-007-9099-9 (2008).
24 Niederkorn, J. Y. High-risk corneal allografts and why they lose their immune privilege. *Curr Opin Allergy Clin Immunol* **10**, 493-497, doi:10.1097/ACI.0b013e32833dfa11 (2010).
25 The collaborative corneal transplantation studies (CCTS). Effectiveness of histocompatibility matching in high-risk corneal transplantation. The Collaborative Corneal Transplantation Studies Research Group. *Arch Ophthalmol* **110**, 1392-1403 (1992).
26 Cursiefen, C., Chen, L., Dana, M. R. & Streilein, J. W. Corneal lymphangiogenesis: evidence, mechanisms, and implications for corneal transplant immunology. *Cornea* **22**, 273-281 (2003).
27 Yamagami, S., Dana, M. R. & Tsuru, T. Draining lymph nodes play an essential role in alloimmunity generated in response to high-risk corneal transplantation. *Cornea* **21**, 405-409 (2002).
28 Yamagami, S. & Dana, M. R. The critical role of lymph nodes in corneal alloimmunization and graft rejection. *Invest Ophthalmol Vis Sci* **42**, 1293-1298 (2001).
29 Dietrich, T. *et al.* Cutting edge: lymphatic vessels, not blood vessels, primarily mediate immune rejections after transplantation. *J Immunol* **184**, 535-539, doi:10.4049/jimmunol.0903180 (2010).
30 Zhang, H., Grimaldo, S., Yuen, D. & Chen, L. Combined blockade of VEGFR-3 and VLA-1 markedly promotes high-risk corneal transplant survival. *Invest Ophthalmol Vis Sci* **52**, 6529-6535, doi:10.1167/iovs.11-7454 (2011).
31 Ling, S., Qi, C., Li, W., Xu, J. & Kuang, W. Crucial role of corneal lymphangiogenesis for allograft rejection in alkali-burned cornea bed. *Clin Exp Ophthalmol* **37**, 874-883, doi:10.1111/j.1442-9071.2009.02178.x (2009).
32 Tang, X. L., Sun, J. F., Wang, X. Y., Du, L. L. & Liu, P. Blocking neuropilin-2 enhances corneal allograft survival by selectively inhibiting lymphangiogenesis on vascularized beds. *Mol Vis* **16**, 2354-2361 (2010).

33 Feng, J. G. *et al.* Clinicopathological pattern and Annexin A2 and Cdc42 status in patients presenting with differentiation and lymphnode metastasis of esophageal squamous cell carcinomas. *Mol Biol Rep* **39**, 1267-1274, doi:10.1007/s11033-011-0859-2 (2012).
34 Bock, F. *et al.* Novel anti(lymph)angiogenic treatment strategies for corneal and ocular surface diseases. *Prog Retin Eye Res* **34**, 89-124, doi:10.1016/j.preteyeres.2013.01.001 (2013).
35 Abdelfattah, N. S., Amgad, M., Zayed, A. A., Hussein, H. & Abd El-Baky, N. Molecular underpinnings of corneal angiogenesis: advances over the past decade. *Int J Ophthalmol* **9**, 768-779, doi:10.18240/ijo.2016.05.24 (2016).
36 Cao, R. *et al.* Collaborative interplay between FGF-2 and VEGF-C promotes lymphangiogenesis and metastasis. *Proc Natl Acad Sci U S A* **109**, 15894-15899, doi:10.1073/pnas.1208324109 (2012).
37 Cursiefen, C. *et al.* VEGF-A stimulates lymphangiogenesis and hemangiogenesis in inflammatory neovascularization via macrophage recruitment. *J Clin Invest* **113**, 1040-1050, doi:10.1172/JCI20465 (2004).
38 Voiculescu, O. B., Voinea, L. M. & Alexandrescu, C. Corneal neovascularization and biological therapy. *J Med Life* **8**, 444-448 (2015).
39 Karpanen, T. & Alitalo, K. Molecular biology and pathology of lymphangiogenesis. *Annu Rev Pathol* **3**, 367-397, doi:10.1146/annurev.pathmechdis.3.121806.151515 (2008).
40 Veikkola, T. *et al.* Signalling via vascular endothelial growth factor receptor-3 is sufficient for lymphangiogenesis in transgenic mice. *EMBO J* **20**, 1223-1231, doi:10.1093/emboj/20.6.1223 (2001).
41 Adams, R. H. & Alitalo, K. Molecular regulation of angiogenesis and lymphangiogenesis. *Nat Rev Mol Cell Biol* **8**, 464-478, doi:10.1038/nrm2183 (2007).
42 Bock, F. *et al.* Blockade of VEGFR3-signalling specifically inhibits lymphangiogenesis in inflammatory corneal neovascularisation. *Graefes Arch Clin Exp Ophthalmol* **246**, 115-119, doi:10.1007/s00417-007-0683-5 (2008).
43 Chen, L. *et al.* Vascular endothelial growth factor receptor-3 mediates induction of corneal alloimmunity. *Nat Med* **10**, 813-815, doi:10.1038/nm1078 (2004).
44 Kubo, H. *et al.* Blockade of vascular endothelial growth factor receptor-3 signaling inhibits fibroblast growth factor-2-induced lymphangiogenesis in mouse cornea. *Proc Natl Acad Sci U S A* **99**, 8868-8873, doi:10.1073/pnas.062040199 (2002).
45 Avraamides, C. J., Garmy-Susini, B. & Varner, J. A. Integrins in angiogenesis and lymphangiogenesis. *Nat Rev Cancer* **8**, 604-617, doi:10.1038/nrc2353 (2008).
46 Altiok, E. *et al.* Integrin Alpha-9 Mediates Lymphatic Valve Formation in Corneal Lymphangiogenesis. *Invest Ophthalmol Vis Sci* **56**, 6313-6319, doi:10.1167/iovs.15-17509 (2015).
47 Sabin, F. R. On the origin of the lymphatic system from the veins, and the development of the lymph hearts and thoracic duct in the pig. *Developmental Dynamics* **1**, 367-389 (1902).

48 Huntington, G. S. & McClure, C. F. W. The anatomy and development of the jugular lymph sacs in the domestic cat (Felis domestica). *Developmental Dynamics* **10**, 177-312 (1910).
49 Klotz, L. *et al.* Cardiac lymphatics are heterogeneous in origin and respond to injury. *Nature* **522**, 62-67, doi:10.1038/nature14483 (2015).
50 Nicenboim, J. *et al.* Lymphatic vessels arise from specialized angioblasts within a venous niche. *Nature* **522**, 56-61, doi:10.1038/nature14425 (2015).
51 Martinez-Corral, I. *et al.* Nonvenous origin of dermal lymphatic vasculature. *Circ Res* **116**, 1649-1654, doi:10.1161/CIRCRESAHA.116.306170 (2015).
52 Stanczuk, L. *et al.* cKit Lineage Hemogenic Endothelium-Derived Cells Contribute to Mesenteric Lymphatic Vessels. *Cell Rep*, doi:10.1016/j.celrep.2015.02.026 (2015).
53 Cao, R. *et al.* Hepatocyte growth factor is a lymphangiogenic factor with an indirect mechanism of action. *Blood* **107**, 3531-3536, doi:10.1182/blood-2005-06-2538 (2006).
54 He, Y. *et al.* Preexisting lymphatic endothelium but not endothelial progenitor cells are essential for tumor lymphangiogenesis and lymphatic metastasis. *Cancer Res* **64**, 3737-3740, doi:10.1158/0008-5472.CAN-04-0088 (2004).
55 Karkkainen, M. J. *et al.* Vascular endothelial growth factor C is required for sprouting of the first lymphatic vessels from embryonic veins. *Nat Immunol* **5**, 74-80, doi:10.1038/ni1013 (2004).
56 Nagy, J. A. *et al.* Vascular permeability factor/vascular endothelial growth factor induces lymphangiogenesis as well as angiogenesis. *J Exp Med* **196**, 1497-1506 (2002).
57 Cimpean, A. M. & Raica, M. Lymphangiogenesis and Inflammation-Looking for the "Missing Pieces" of the Puzzle. *Arch Immunol Ther Exp (Warsz)* **63**, 415-426, doi:10.1007/s00005-015-0349-7 (2015).
58 Tan, K. W., Chong, S. Z. & Angeli, V. Inflammatory lymphangiogenesis: cellular mediators and functional implications. *Angiogenesis* **17**, 373-381, doi:10.1007/s10456-014-9419-4 (2014).
59 Kim, H., Kataru, R. P. & Koh, G. Y. Inflammation-associated lymphangiogenesis: a double-edged sword? *J Clin Invest* **124**, 936-942, doi:10.1172/JCI71607 (2014).
60 Salven, P., Mustjoki, S., Alitalo, R., Alitalo, K. & Rafii, S. VEGFR-3 and CD133 identify a population of CD34+ lymphatic/vascular endothelial precursor cells. *Blood* **101**, 168-172, doi:10.1182/blood-2002-03-0755 (2003).
61 Kerjaschki, D. *et al.* Lymphatic endothelial progenitor cells contribute to de novo lymphangiogenesis in human renal transplants. *Nat Med* **12**, 230-234, doi:10.1038/nm1340 (2006).
62 Maruyama, K. *et al.* Inflammation-induced lymphangiogenesis in the cornea arises from CD11b-positive macrophages. *J Clin Invest* **115**, 2363-2372, doi:10.1172/JCI23874 (2005).
63 Conrad, C. *et al.* Multipotent mesenchymal stem cells acquire a lymphendothelial phenotype and enhance lymphatic regeneration in vivo. *Circulation* **119**, 281-289, doi:10.1161/CIRCULATIONAHA.108.793208 (2009).

64 Zumsteg, A. *et al.* Myeloid cells contribute to tumor lymphangiogenesis. *PLoS One* **4**, e7067, doi:10.1371/journal.pone.0007067 (2009).
65 Park, J. H. *et al.* Endothelial progenitor cell transplantation decreases lymphangiogenesis and adverse myocardial remodeling in a mouse model of acute myocardial infarction. *Exp Mol Med* **43**, 479-485, doi:10.3858/emm.2011.43.8.054 (2011).
66 Hall, K. L., Volk-Draper, L. D., Flister, M. J. & Ran, S. New model of macrophage acquisition of the lymphatic endothelial phenotype. *PLoS One* **7**, e31794, doi:10.1371/journal.pone.0031794 (2012).
67 Tawada, M., Hayashi, S., Osada, S., Nakashima, S. & Yoshida, K. Human gastric cancer organizes neighboring lymphatic vessels via recruitment of bone marrow-derived lymphatic endothelial progenitor cells. *J Gastroenterol* **47**, 1057-1060, doi:10.1007/s00535-012-0638-4 (2012).
68 Tawada, M., Hayashi, S., Ikegame, Y., Nakashima, S. & Yoshida, K. Possible involvement of tumor-producing VEGF-A in the recruitment of lymphatic endothelial progenitor cells from bone marrow. *Oncol Rep* **32**, 2359-2364, doi:10.3892/or.2014.3499 (2014).
69 Tan, Y. Z. *et al.* CD34+ VEGFR-3+ progenitor cells have a potential to differentiate towards lymphatic endothelial cells. *J Cell Mol Med* **18**, 422-433, doi:10.1111/jcmm.12233 (2014).
70 DiMaio, T. A., Wentz, B. L. & Lagunoff, M. Isolation and characterization of circulating lymphatic endothelial colony forming cells. *Exp Cell Res* **340**, 159-169, doi:10.1016/j.yexcr.2015.11.015 (2016).
71 Buttler, K., Lohrberg, M., Gross, G., Weich, H. A. & Wilting, J. Integration of CD45-positive leukocytes into newly forming lymphatics of adult mice. *Histochem Cell Biol* **145**, 629-636, doi:10.1007/s00418-015-1399-y (2016).
72 Alunno, A. *et al.* Mobilization of lymphatic endothelial precursor cells and lymphatic neovascularization in primary Sjogren's syndrome. *J Cell Mol Med* **20**, 613-622, doi:10.1111/jcmm.12793 (2016).
73 Beerens, M. *et al.* Multipotent Adult Progenitor Cells Support Lymphatic Regeneration at Multiple Anatomical Levels during Wound Healing and Lymphedema. *Sci Rep* **8**, 3852, doi:10.1038/s41598-018-21610-8 (2018).
74 Schniedermann, J. *et al.* Mouse lung contains endothelial progenitors with high capacity to form blood and lymphatic vessels. *BMC Cell Biol* **11**, 50, doi:10.1186/1471-2121-11-50 (2010).
75 Cimini, M., Cannata, A., Pasquinelli, G., Rota, M. & Goichberg, P. Phenotypically heterogeneous podoplanin-expressing cell populations are associated with the lymphatic vessel growth and fibrogenic responses in the acutely and chronically infarcted myocardium. *PLoS One* **12**, e0173927, doi:10.1371/journal.pone.0173927 (2017).
76 Religa, P. *et al.* Presence of bone marrow-derived circulating progenitor endothelial cells in the newly formed lymphatic vessels. *Blood* **106**, 4184-4190, doi:10.1182/blood-2005-01-0226 (2005).
77 Lee, J. Y. *et al.* Podoplanin-expressing cells derived from bone marrow play a crucial role in postnatal lymphatic neovascularization. *Circulation* **122**, 1413-1425, doi:10.1161/CIRCULATIONAHA.110.941468 (2010).

78 Choi, I. *et al.* Visualization of lymphatic vessels by Prox1-promoter directed GFP reporter in a bacterial artificial chromosome-based transgenic mouse. *Blood* **117**, 362-365, doi:10.1182/blood-2010-07-298562 (2011).
79 Kang, G. J. *et al.* Intravital Imaging Reveals Dynamics of Lymphangiogenesis and Valvulogenesis. *Sci Rep* **6**, 19459, doi:10.1038/srep19459 (2016).
80 Grimaldo, S., Yuen, D., Ecoiffier, T. & Chen, L. Very late antigen-1 mediates corneal lymphangiogenesis. *Invest Ophthalmol Vis Sci* **52**, 4808-4812, doi:10.1167/iovs.10-6580 (2011).
81 Choi, I. *et al.* 9-cis retinoic acid promotes lymphangiogenesis and enhances lymphatic vessel regeneration: therapeutic implications of 9-cis retinoic acid for secondary lymphedema. *Circulation* **125**, 872-882, doi:10.1161/CIRCULATIONAHA.111.030296 (2012).
82 Yuen, D. *et al.* Live imaging of newly formed lymphatic vessels in the cornea. *Cell Res* **21**, 1745-1749, doi:10.1038/cr.2011.178 (2011).
83 Zhang, L. *et al.* Angiopoietin-2 Blockade Promotes Survival of Corneal Transplants. *Invest Ophthalmol Vis Sci* **58**, 79-86, doi:10.1167/iovs.16-20485 (2017).
84 Yuen, D., Pytowski, B. & Chen, L. Combined blockade of VEGFR-2 and VEGFR-3 inhibits inflammatory lymphangiogenesis in early and middle stages. *Invest Ophthalmol Vis Sci* **52**, 2593-2597, doi:10.1167/iovs.10-6408 (2011).
85 Yuen, D. *et al.* Role of angiopoietin-2 in corneal lymphangiogenesis. *Invest Ophthalmol Vis Sci* **55**, 3320-3327, doi:10.1167/iovs.13-13779 (2014).
86 Schneider, C. A., Rasband, W. S. & Eliceiri, K. W. NIH Image to ImageJ: 25 years of image analysis. *Nat Methods* **9**, 671-675 (2012).
87 Chen, L., Hann, B. & Wu, L. Experimental models to study lymphatic and blood vascular metastasis. *J Surg Oncol* **103**, 475-483, doi:10.1002/jso.21794 (2011).
88 Zecevic, N. & Rakic, P. Synaptogenesis in monkey somatosensory cortex. *Cereb Cortex* **1**, 510-523 (1991).
89 Folkman, J. Tumor angiogenesis: therapeutic implications. *N Engl J Med* **285**, 1182-1186, doi:10.1056/NEJM197111182852108 (1971).
90 Dashkevich, A. *et al.* Lymph angiogenesis after lung transplantation and relation to acute organ rejection in humans. *Ann Thorac Surg* **90**, 406-411, doi:10.1016/j.athoracsur.2010.03.013 (2010).
91 Stuht, S. *et al.* Lymphatic neoangiogenesis in human renal allografts: results from sequential protocol biopsies. *Am J Transplant* **7**, 377-384 (2007).
92 Geissler, H. J. *et al.* First year changes of myocardial lymphatic endothelial markers in heart transplant recipients. *Eur J Cardiothorac Surg* **29**, 767-771, doi:10.1016/j.ejcts.2005.12.024 (2006).
93 Ecoiffier, T., Yuen, D. & Chen, L. Differential distribution of blood and lymphatic vessels in the murine cornea. *Invest Ophthalmol Vis Sci* **51**, 2436-2440, doi:10.1167/iovs.09-4505 (2010).
94 Bazigou, E. *et al.* Integrin-alpha9 is required for fibronectin matrix assembly during lymphatic valve morphogenesis. *Dev Cell* **17**, 175-186, doi:10.1016/j.devcel.2009.06.017 (2009).

95 Huang, X. Z. *et al.* Fatal bilateral chylothorax in mice lacking the integrin alpha9beta1. *Mol Cell Biol* **20**, 5208-5215 (2000).
96 Chen, W. S. *et al.* Pathological lymphangiogenesis is modulated by galectin-8-dependent crosstalk between podoplanin and integrin-associated VEGFR-3. *Nat Commun* **7**, 11302, doi:10.1038/ncomms11302 (2016).
97 Kang, G. J. *et al.* Integrin Alpha 9 Blockade Suppresses Lymphatic Valve Formation and Promotes Transplant Survival. *Invest Ophthalmol Vis Sci* **57**, 5935-5939, doi:10.1167/iovs.16-20130 (2016).